Anisotropy dependent Relaxation of Topologically-modified polymers

A Thesis

submitted to
Indian Institute of Science Education and Research Pune
in partial fulfillment of the requirements for the
BS-MS Dual Degree Programme

by

Dhruv Patel

Indian Institute of Science Education and Research Pune
Dr. Homi Bhabha Road,
Pashan, Pune 411008, INDIA.

May, 2025

Supervisor: Dr. Apratim Chatterji

Certificate

This is to certify that this dissertation entitled Anisotropy dependent Relaxation of Topologically-modified polymerstowards the partial fulfilment of the BS-MS dual degree programme at the Indian Institute of Science Education and Research, Pune represents study/work carried out by Dhruv Patelat Indian Institute of Science Education and Research under the supervision of Dr. Apratim Chatterji, Associate Professor, Department of Physics , during the academic year 2020-2025.

Dr. Apratim Chatterji

Committee:

Dr. Apratim Chatterji

Dr. Arijit Bhattacharyay

"A theory, or, more concretely, a model, of a mechanism is not a description of reality; it is a description of our assumptions about reality"

- Jeremy Gunawardena

Declaration

I hereby declare that the matter embodied in the report entitled Anisotropy dependent Relaxation of Topologically-modified polymers are the results of the work carried out by me at the Department of Physics, Indian Institute of Science Education and Research, Pune, under the supervision of Dr. Apratim Chatterji and the same has not been submitted elsewhere for any other degree.

Dhruv Patel

Acknowledgments

This Master's thesis marks the final stage of the five-year journey at IISER Pune and it wouldn't have been possible without presence of several individuals.

Firstly, I would like to thank my supervisor Prof. Apratim Chatterji for being an invaluable support during my thesis and giving me freedom to work at my own pace. I was able to explore a lot of new ideas by talking to him, as well as the group including Harsh, Shreerang, Shailesh, Kingkini, and Om who made my life so much easier and fun in the lab. I would also like to thank my previous projects supervisors Prof. Arijit and Prof. Madhusudhan for being such wonderful people and always willing to advice me both academically and non-academically whenever I needed. From all of them I learnt the most important thing- how to think about a research problem.

I am indebted to Mummy and Daddy for giving me freedom to figure out my own path from childhood and make my own mistakes, and honestly that is the most I could have asked for. Their support and encouragement have been truly precious.
Thanks to Rakesh Sir and Priya teacher for being the best mentors and teachers. I would like to thank Dev, Zeal, Ayush and Harsh for constantly being there from home whenever I called, even though we barely met you all were never unapproachable.

I met so many wonderful people who became my family and made IISER my home away from home. I would like to start by thanking my roommate Dhruv, choosing him is probably the best decision I have taken in my life. I would also like to thank my friends Sayan, Aaditya, Gaurav, Kwanit, Vinayak, Goraksh, Shreya, Oyindrila, and Shinjini with whom I have made so many memories during my time here and I am sure many more to come in the future. Mimamsa was a huge part of my time here through which I made wonderful friends- Amogh, Soumil, Kaustubh and Dhairya, these people greatly influenced my way of thinking about

a problem and Science in general. I would also like to thank Gaurang and Debarghya with whom I had endless debates and discussions on probably every possible thing out there. Shoutout to whole LKG cricket team for including me in their cohort, never felt like a senior.

Now I would like to thank my other family where everyone became very close to each other in the span of last 2 years. Aneri, Raksha, Rushik, Nisarg and Satra - thank you for making Navratri at IISER so much special. Thank you for this friendship which I am asssuming/demanding is only going to stay and grow stronger.

So much to say to all these people, but cannot find words. Then would just end on a poetic note " Kitne khoobsurat thein ye lamhein, ye batane ko shabd mil jaayein, toh kya khaak khoobsurat thein ye lamhein ".

Abstract

This thesis is an investigation of relaxation dynamics of topologically modified polymers. We work with modified ring polymer systems whose importance have been shown in previous work where these topologies are able to explain the spatiotemporal organization of the chromosome inside the E.Coli bacterial cell. The effect of these polymer topologies on the emergent properties and dynamics of the chromosomes is yet unknown. In order to understand that, one first needs to understand the dynamical properties of the individual topologically modified polymers and how cross-links affect these properties. This demands a more robust and systematic study of the dynamics of these complex systems. Herein, we will also present the shortcomings of the End-to-End vectors method to study the relaxation time of the polymers because of the ambiguity that arises while choosing vectors in more complicated topologies. Then I will present two global methods to study the dynamics. Importantly, these global methods - the correlation in fluctuations of radius of gyration and time autocorrelation of eigenvectors of gyration tensor - does not depend on the intricate structural/topological details of the polymer topology. And hence, provides us a mechanism to study any form of complex topology by overcoming the problems with end-to-end vector method. Later in the thesis we also explain the properties of the relaxation dynamics for different ratios of Dumbbell architecture (two loops formed by adding a crosslink between two monomers of ring polymer) and Arc1_2 architectures (three loops formed via adding two additional cross links in ring polymer) by correlating it with the Anisotropy or the asphericity of the polymer. This also lead us to a scaling relation between the relaxation time and Anisotropy of the polymer.

Contents

Chapter 1

Introduction

1.1 Soft Matter: Definition and its applications

Condensed Matter physics provides a structured framework to understand collective assemblies of materials by means of interaction between the constituents of the system. Soft Matter physics is a part of Condensed Matter physics that tries to explain the properties of "soft" class of materials. As the name suggests, these materials are easily deformable in the presence of an external force compared to solid state systems, but they also aren't like simple liquids in a sense that they still maintain structural integrity. This contrast arises due to the weak nature of intermolecular forces that are present instead of strong forces that are often present in crystalline solids. The constituent building blocks are also larger in size as the properties studied are at mesoscale length scales (nanometers to microns). As we are looking at such relatively large length scales, quantum effects can be ignored while studying these systems. The interaction energy in soft materials is of the same order as room-temperature thermal energies; thus, thermal fluctuations are also dominant and play an important role in investigating such systems. Often tools from equilibrium and non-equilibrium statistical mechanics are used to study soft matter systems.

Some examples of soft matter include foam, gels, polymers, colloids, liquid crystals, granular materials, etc. These materials have several applications in our everyday life. For example, toothpaste, ketchup, shaving gels, painting colors, human blood, milk, soaps, etc. are soft matter systems. Additionally, soft matter also include biological systems like membranes,

tissues, chromosomes, etc. The use of soft matter physics in understanding, modeling and theorizing physical principles to understanding these biological systems has been a vital factor for the boom of soft matter physics in the past two decades.

The characteristic of self-assembly shown by these soft matter make them extremely interesting to study. Since these soft matter are constantly undergoing Brownian motion where they tend to move towards equilibrium. They never reach equilibrium in the case of non-equilibrium driven systems because they receive energy at each step. The equilibrium state with lowest free energy is achieved via an intricate balance between the energy and the entropy of the system. This leads to a very rich phase space behavior showcasing spontaneous self-organization of complex structures.

At equilibrium these systems reach equilibrium by minimizing the Helmholtz Free Energy given by:

$$F = U - TS \tag{1.1}$$

Here 'U' is the internal energy, 'T' is the temperature of the system and 'S' is the entropy of the system. Since soft matter systems have internal energy comparable to 'TS' there is a delicate balance between 'U' and 'TS' that determines the equilibrium state of the system.

This self-assembly can also take place hierarchically where molecules self-assemble to form supramolecular structures, which again self assemble to form higher order structures. One such example is the chromosome in the condensed state where there are several orders of hierarchal self-assembly. There are synthetic self-assembled structures as well which have found their use in many industrial applications like the fabrication of nano-devices and nano-materials. This makes the research to understand these self-assembling structures all the more essential.

1.2 History of Soft Matter

The first experimental observation of statistical physics dates back to early 18th century when Robert Brown, a botanist, in 1827, observed the random motion of pollen grains in water which is now referred to as Brownian motion. Later, in early 19th century, Albert

Einstein and Marian Smoluchowski independently laid down the theoretical foundations to understand Brownian motion. They proposed that the energy of the Brownian particle is similar to the fluid it is suspended in. This lead to foundational understanding of the systems now referred to as colloids. Their work also lead the way to significant advancements in the field of Statistical Mechanics. In 1920, Hermann Staudinger proposed the idea of macromolecule for the first time by suggesting that polymers are formed by linking molecules together by covalent bonds. He also received Nobel Prize in Chemistry in 1953. In the same decade, the use of hygrogel in biomedical sciences was pioneered by Drahoslav Lim and Otto Wichterle.

These seemingly different fields were brought together under the same umbrella by Pierre-Gilles de Gennes. He was awarded the Nobel Prize in Physics in the year 1991 "for discovering that methods developed for studying order phenomena in simple systems can be generalized to more complex forms of matter, in particular to liquid crystals and polymers." His work showed that the physics lying beneath these different chemical and biological systems is the universal property of these soft matter systems. He also did seminal work and extended the understanding of phase changes in liquid crystals and polymers. From the early 21st century, the field of soft matter has gained prominence for its role in studying complex biological systems. This has led to an interesting branch of soft matter called Biological Physics or Physics of Living Systems.

1.3 Polymer Physics

Polymer Physics, a branch of soft matter physics, is the study of structural and dynamical properties of large macromolecules composed of repeating subunits called monomers. For Physicists, they often study coarse-grained model of polymeric systems. So for them one repeating subunit or monomer in this coarse grained description can represent many chemical subunits of the macromolecule or polymer. We do this coarse graining since we are interested in the universal properties of the system rather than chemical properties.

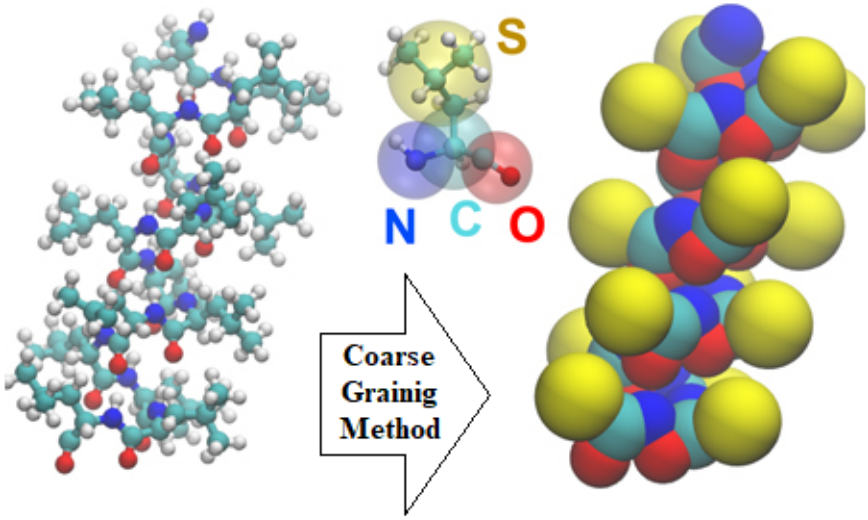

Figure 1.1: The figure represents the process of coarse-graining of a polymer model.

Statistical Mechanics lie at the very core of the theoretical framework of polymer physics. Tools from equilibrium and non-equilibrium statistical mechanics have been extensively used to understand structural and dynamical properties of these polymeric systems. These polymers are long chains of repeating subunits which can take several conformation in the phase space which contributes to the entropy of the system. As the number of monomers increases so does the number of possible configurations and consequently the entropy associated with the system. In the literature of polymer physics, there exists several models to study the conformations of these polymer systems like the freely jointed chain model, the worm-like model, etc. All of these models deal with different type of conformations a polymer chain may take. There is also well developed theory for the effect of excluded volume on the conformation of the polymer. Excluded volume takes into account the fact that two monomers cannot come very close to each other and hence some volume surrounding one monomer is prohibited for every other monomer in the system. This property of excluded volume also has effects on the entropy, organization and dynamics of the system. There also exists reptation model, which as the name suggests, describes the snake-like motion of a polymer chain in a very dense system where it is surrounded by many other polymers. Such dense systems are called melts. By using tools from statistical mechanics, one can make accurate predictions about the size and dynamics of linear polymer chain. However, for complicated topologies of

polymer architectures there doesn't exist a complete theoretical and computational studies and that is where this thesis comes in where we try to explain dynamics of these complicated topologies using a generalized framework.

1.4 Polymer as a self-avoiding Random Walk

A polymer can be treated as a self-avoiding random walk in three dimensions where every step you take, you place a bead, and connect it to the previous bead, with the condition that you cannot arrive at the same coordinates more than once.

1.4.1 Size of a Polymer

As the polymer diffuses over time and reaches an equilibrium conformation, its equilibrium size can be estimated by measuring the mean squared end-to-end distance. In case of an ideal linear chain, i.e. when the excluded volume interaction is absent, the mean squared end-to-end distance is calculated as follows:

$$\left\langle R^2 \right\rangle = \left\langle \vec{R_n} \cdot \vec{R_n} \right\rangle = \sum_{i=1}^{n} \sum_{j=1}^{n} \langle \vec{r_i} \cdot \vec{r_j} \rangle \tag{1.2}$$

where $\vec{R_n}$ is the end-to-end vector of a polymer chain.

1.4.2 Freely Rotating Chain model

In order to solve the above equation we need to find the correlation between bond vectors $\vec{r_i}$ and $\vec{r_j}$. For the case of freely rotating chain model, the correlation between the component of vector $\vec{r_j}$ perpendicular to vector $\vec{r_{j-1}}$ on average will be zero because the vector can point in any direction with torsion angle ϕ_j since it is a freely rotating chain.

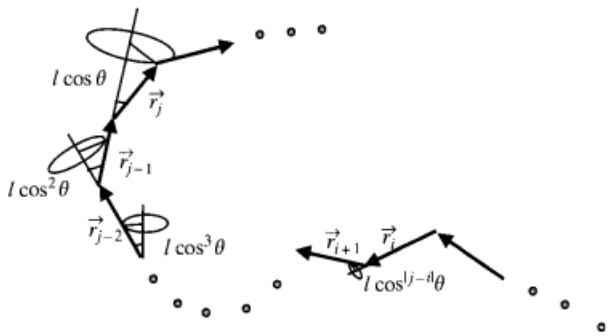

Figure 1.2: The figure represents bond vectors and their correlations with adjacent bond vectors.

So, only the component of $\vec{r_j}$ along the direction of vector $\vec{r_{j-1}}$ i.e. $l\cos\theta$ contributes to the average of correlation. Similarly this correlation is passed down by bond vector $\vec{r_{j-1}}$ to vector $\vec{r_{j-2}}$ as $l\cos^2\theta$. Thus the correlation between vectors $\vec{r_i}$ and $\vec{r_j}$ is

$$\langle \vec{r_i} \cdot \vec{r_j} \rangle = l^2(\cos\theta)^{|j-1|} \tag{1.3}$$

The mean squared end-to-end distance can also be written as

$$\left\langle R^2 \right\rangle = \sum_{i=1}^{n}\sum_{j=1}^{n} \langle \vec{r_i} \cdot \vec{r_j} \rangle = \sum_{i=1}^{n}\left(\sum_{j=1}^{i-1} \langle \vec{r_i} \cdot \vec{r_j} \rangle + \left\langle \vec{r_i}^2 \right\rangle + \sum_{j=i+1}^{n} \langle \vec{r_i} \cdot \vec{r_j} \rangle\right) \tag{1.4}$$

$$= \sum_{i=1}^{n} \left\langle \vec{r_i}^2 \right\rangle + l^2 \sum_{i=1}^{n}\left(\sum_{j=1}^{i-1} (\cos\theta)^{i-j} + \sum_{j=i+1}^{n} (\cos\theta)^{j-i}\right) \tag{1.5}$$

$$= nl^2 + l^2 \sum_{i=1}^{n}\left(\sum_{k=1}^{i-1} \cos^k\theta + \sum_{k=1}^{n-i} \cos^k\theta\right) \tag{1.6}$$

Here the term $(\cos\theta)^{|j-i|}$ decays rapidly with increasing the number of bonds between bond vectors $\vec{r_j}$ and $\vec{r_i}$.

$$(\cos\theta)^{|j-i|} = exp\left[|j-i|ln(\cos\theta)\right] = exp\left[-\frac{|j-i|}{s_p}\right] \tag{1.7}$$

$$s_p = -\frac{1}{ln(\cos\theta)} \tag{1.8}$$

Here s_p is defined as the number of main chain bonds in the persistence segment of the polymer chain. It gives a quantitative measure of the scale at which bond correlations decay. Taking this rapid decay into account one can proceed solving equation (1.6) above as follows

$$\sum_{i=1}^{n}\left(\sum_{k=1}^{i-1}\cos^k\theta + \sum_{k=1}^{n-i}\cos^k\theta\right) \approx 2\sum_{i=1}^{n}\sum_{k=1}^{\infty}\cos^k\theta = 2n\sum_{k=1}^{\infty}\cos^k\theta \tag{1.9}$$

$$= 2n\frac{\cos\theta}{1-\cos\theta} \tag{1.10}$$

This gives the mean squared end-to-end distance for a freely rotating chain model as

$$\left\langle R^2\right\rangle = nl^2 + 2nl^2\frac{\cos\theta}{1-\cos\theta} = nl^2\frac{1+\cos\theta}{1-\cos\theta} \tag{1.11}$$

Here we get the mean squared end-to-end distance as a simple function of number of bonds in the polymer chain n, length of each bond l, and the bond angle θ

1.4.3 Worm-like chain model

The worm-like chain model or the Kratky-Porod model is a special case of freely-jointed chain model when the bond angle θ takes very small values. This model has been used to study stiff polymeric systems like the double-stranded DNA. For small values of θ one can

expand $\cos\theta$ about $\theta = 0$:

$$\cos\theta \approx 1 - \frac{\theta^2}{2} \tag{1.12}$$

For small y, $ln(1-y) \approx -y$,

$$ln(\cos\theta \approx -\frac{\theta^2}{2} \tag{1.13}$$

As θ is small, the persistence segment can be written as

$$s_p = -\frac{1}{ln(\cos\theta} \approx \frac{2}{\theta^2} \tag{1.14}$$

The persistence length is the measure of length of persistence segment and is given by

$$l_p = s_p l = l\frac{2}{\theta^2} \tag{1.15}$$

For a real biological example, the persistence length of a double helical DNA is known to be around $\approx 50\ nm$. Here one can directly see the importance and power of tools of statistical mechanics in describing biological system.

1.4.4 Radius of Gyration of Polymer chain

In the previous subsections, we looked at mean squared end-to-end distance to measure the size of polymer. But end-to-end vectors do not give an accurate prediction of the volume occupied by the polymer since it spans a very large volume . Instead a better quantity if

radius of gyration, which takes into account the distance of each monomer from the center of mass of the polymer chain. Additionally, end-to-end vectors can only be described in case of a linear polymer chain, but for more complicated topologies like branched polymers or even ring polymers, end-to-end vectors cannot be defined. Hence we need a general quantity to measure the size of polymer. The square radius of gyration is defined as the average of square of distance between monomers and the center of mass of polymer at a given conformation:

$$R_g^2 = \frac{1}{N}\sum_{i=1}^{N}\left(\vec{R_i} - \vec{R_{cm}}\right)^2 \tag{1.16}$$

$$\vec{R_{cm}} = \frac{1}{N}\sum_{j=1}^{N}\vec{R_j} \tag{1.17}$$

here N is the total number of monomers and $\vec{R_{cm}}$ is the center of mass of polymer. Substituting $\vec{R_{cm}}$ in the above equation we get:

$$R_g^2 = \frac{1}{N}\sum_{i=1}^{N}\left(\vec{R_i}^{\,2} - 2\vec{R_i}\vec{R_{cm}} + \vec{R_{cm}}^{\,2}\right) \tag{1.18}$$

$$= \frac{1}{N}\sum_{i=1}^{N}\left[\vec{R_i}^{\,2}\frac{1}{N}\sum_{j=1}^{N}1 - 2\vec{R_i}\frac{1}{N}\sum_{j=1}^{N}\vec{R_j} + \left(\frac{1}{N}\sum_{j=1}^{N}\vec{R_j}\right)^2\right] \tag{1.19}$$

The last term can be written as:

$$\frac{1}{N}\sum_{i=1}^{N}\left(\frac{1}{N}\sum_{j=1}^{N}\vec{R_j}^{\,2}\right)=\left(\frac{1}{N}\sum_{j=1}^{N}\vec{R_j}^{\,2}\right)=\left(\frac{1}{N}\sum_{i=1}^{N}\vec{R_i}\right)\left(\frac{1}{N}\sum_{i=j}^{N}\vec{R_j}\right) \tag{1.20}$$

$$=\frac{1}{N^2}\sum_{i=1}^{N}\sum_{j=1}^{N}\vec{R_i}\vec{R_j} \tag{1.21}$$

Substituting this in equation 1.19 gives:

$$R_g^2=\frac{1}{N^2}\sum_{i=1}^{N}\sum_{j=1}^{N}\left(\vec{R_i}^{\,2}-2\vec{R_i}\vec{R_j}+\vec{R_i}\vec{R_j}\right)=\frac{1}{N^2}\sum_{i=1}^{N}\sum_{j=1}^{N}\left(\vec{R_i}^{\,2}-\vec{R_i}\vec{R_j}\right) \tag{1.22}$$

$$=\frac{1}{2}\left[\frac{1}{N^2}\sum_{i=1}^{N}\sum_{j=1}^{N}\left(\vec{R_i}^{\,2}-\vec{R_i}\vec{R_j}\right)+\frac{1}{N^2}\sum_{j=1}^{N}\sum_{i=1}^{N}\left(\vec{R_j}^{\,2}-\vec{R_j}\vec{R_i}\right)\right] \tag{1.23}$$

$$=\frac{1}{2N^2}\sum_{i=1}^{N}\sum_{j=1}^{N}\left(\vec{R_i}-\vec{R_j}\right)^2 \tag{1.24}$$

Now since each pair of monomers enter the summation twice, we can write the above equation with only considering one pair in summation once as:

$$R_g^2=\frac{1}{N^2}\sum_{i=1}^{N}\sum_{j=1}^{N}\left(\vec{R_i}-\vec{R_j}\right)^2 \tag{1.25}$$

$$\left\langle R_g^2\right\rangle=\frac{1}{N}\sum_{i=1}^{N}\left\langle\left(\vec{R_i}-\vec{R_{cm}}\right)^2\right\rangle=\frac{1}{N^2}\sum_{i=1}^{N}\sum_{j=1}^{N}\left\langle\left(\vec{R_i}-\vec{R_j}\right)^2\right\rangle \tag{1.26}$$

Now using this equation we can calculate radius of gyration for a ideal linear polymer chain. In order to do this, we can replace summation over monomers by integrals along contours of the chain by replacing monomer indices i and j with continuous coordinates u and v :

$$\sum_{i=1}^{N} = \int_0^N du \tag{1.27}$$

$$\sum_{j=i}^{N} = \int_u^N dv \tag{1.28}$$

The mean square distance between points u and v on contour can be obtained by treating it as an ideal chain of $v-u$ monomers. Thus the integral takes the form

$$\left\langle R_g^2 \right\rangle = \frac{1}{N^2} \int_0^N \int_u^N \left\langle \left(\vec{R(u)} - \vec{R(v)} \right)^2 \right\rangle dv\, du \tag{1.29}$$

$$\left\langle \left(\vec{R(u)} - \vec{R(v)} \right)^2 \right\rangle = (v-u)b^2 \tag{1.30}$$

Let $v' = v - u$ and $u' = N - u$, then

$$\left\langle R_g^2 \right\rangle = \frac{b^2}{N^2} \int_0^N \int_u^N (v-u)\, dv\, du = \frac{b^2}{N^2} \int_0^N \int_0^{N-u} v'\, dv'\, du \tag{1.31}$$

$$= \frac{b^2}{N^2} \int_0^N \frac{(N-u)^2}{2}\, du = \frac{b^2}{2N^2} \int_0^N (u')^2\, du' = \frac{Nb^2}{6} \tag{1.32}$$

This implies, that for an ideal linear polymer chain

$$\left\langle R_g^2 \right\rangle = \frac{Nb^2}{6} = \frac{\langle R^2 \rangle}{6} \tag{1.33}$$

For a ring polymer this relation comes put to be $\left\langle R_g^2 \right\rangle = \frac{Nb^2}{12}$. Now this relation is for a an ideal case where $R_g \propto N^{0.5}$, but for the case where excluded volume interaction is accounted for $R_g \propto N^{0.6}$.

1.5 Relaxation Dynamics: Definition and Why should we study it?

The physics of topologically modified polymers is important to understand the chromosome organization as well as the spatiotemporal dynamics of chromosomes as they go through their life-cycle. Topological modifications in DNA-polymers occur by loop extrusion or by linker proteins that link promoter and enhancer regions to activate a gene. This is turn creates internal loops with a DNA-polymer. Moreover, chromosome organization is different for different cell types within the same organism. It is expected that different size and position of the loops along the polymer backbone plays an important role to realize different chromosome organizations in different cells.

We have investigated at polymer organization in confinement by designing specific loops along the polymer contour. This was then used to identify the underlying mechanism of bacterial chromosome organization. To obtain insights about the physics of topologically modified polymers we used permanent cross-links (fixed topology) in a bead-spring polymer model. This insight was to model transient loops in replicating chromosomes to explain bacterial chromosome organization.

Thereafter, it is of interest to explore how topological modifications affect the dynamics of polymers. To that end, this thesis is an investigation to understand how topological modifications modifies polymer dynamics. We use specific designer topologies (some of which have been shown to be relevant to chromosome organization) to identify which are the primary factors which determine polymer dynamics of unentangled polymers. It is known that chromosomes maintain chromosome territories inside the nucleus and remain

unentangled. We study single polymer dynamics with excluded volume interactions using Langevin dynamics, as it has been shown that it is sufficient to model dense polymer solutions for small chains.

In order to study dynamics of these polymeric systems, in this thesis we investigate relaxation time of these systems. Global relaxation time τ means the equilibration time of these systems. Beyond this time, the internal motion plays no significant role in the global dynamics of the polymer. This is especially important both in context of polymer physics and chromosome dynamics where modified polymer architectures are used studied because all the meaningful statistical quantities can only be calculated once the system has reached equilibrium. And since there is no theoretical result which talks about timescale for these modified polymers, this study becomes of crucial importance.

1.6 Thesis Outline

In this thesis we first start by a brief investigation of relaxation dynamics using end-to-end vectors for different modified polymer topologies. Then to remove the dependence of a method on the intrinsic topologies of the architecture. we investigate the relaxation dynamics using two global quantities, namely, the correlation in fluctuations of radius of gyration and second the time autocorrelation of eigenvectors of gyration tensor. This study being computational in nature we use Langevin Dynamics simulations of bead-spring polymer models. In our study, we have only dealt with melt conditions and ignored hydrodynamic interactions with solvent which add more complications to the problem. We have used different topologically modified polymers in our study which will described in detail in the next chapter. The studies done in the thesis are as follows:

1. Relaxation time using end-to-end vectors.
2. Relaxation time using correlation in fluctuations of Radius of Gyration that we term as C_g.
3. Relaxation time using time autocorrelation of eigenvectors of Radius of Gyration Tensor that we term as C_E.
4. Investigation of anisotropy of different modified polymer topologies.

5. Scaling law between relaxation time, anisotropy, and number of monomers that we denote by A.

6. Brief study of relaxation time of semi-flexible linear chain.

Chapter 2

Models and Methodology

2.1 Role of Computational Physics

Statistical Mechanics provides a strong theoretical framework for many-body physics. There exist powerful tools to study the phase transitions and static properties of these systems analytically. But in order to study the dynamical properties of these may-body systems which can show interesting emergent properties like spatiotemporal organization, one needs computational methods based on physics. These computational approaches help us to study these systems at various time and length scales. Since the past two decades, people have extensively started looking at atomistic molecular level simulations by leveraging the computational methods. This has enabled modeling and visualization of time evolution of these macromolecular systems.

Molecular Dynamics (MD) and Monte Carlo (MC) methods are two of the most famous physics based computational methods that have been used in various fields of physics from studying large cosmological simulations to various atomistic simulations. Monte Carlo simulation gives insights into static properties of the system without giving any information about the dynamics of the system. MC methods have been extensively used to study phase transitions and thermal properties in classical and quantum lattice models. There are also Quantum Monte Carlo methods to study various complex quantum many-body systems. On the other hand, Molecular Dynamics (MD) Simulations - developed based on the laws of statistical mechanics and classical mechanics, have been used to study dynamical evolution

of the system with time. Molecular Dynamics simulations also give us the ability to study the interaction of the system with environment or surrounding. In case of polymeric systems, the external environment might be solvent in dilute systems, other polymers in melt conditions, or both in the case of semi-dilute systems. Quite often, we study Coarse-Grained (CG) models of these polymers by simulations. In this case, one monomer in our simulation can represent a large number of subunits of a macromolecule. This is advantageous in two ways - first it allows us to study the dynamics and other properties of very large systems and second it reduces the computational expense in terms of time and processing power. Computational approaches have become an integral part of studying phase transitions, dynamics and conformations of polymer systems. In general, computational methods have complemented theoretical and experimental efforts in all the domains of physics. It has become nearly necessary to use computational methods to study complex many-body systems to try and explain experimental data and make further strides in theory.

In my study, I have developed Langevin Dynamics simulations for different topologically modified polymers. For longer chain I have used LAMMPS Molecular Dynamics simulator for calculating relevant quantities. The analysis of this data give us interesting insights into the system which are described in detail in the following chapters of the thesis.

2.2 Computational Model

In the thesis we have looked at bead-spring models of polymers. Here beads basically mean monomers, which are connected via a harmonic spring with their neighboring monomers.

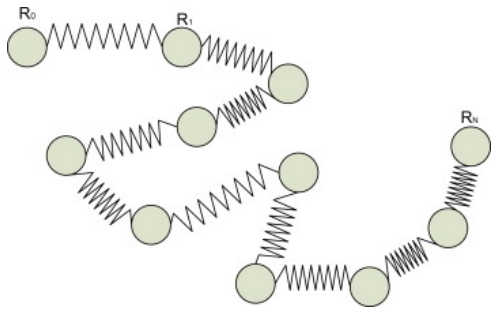

Figure 2.1: The figure represents bead-spring model of a polymer.

For displacement δx the potential energy U stored in spring with spring constant κ is given by:

$$U = \frac{\kappa(\delta x)^2}{2} \tag{2.1}$$

We use Langevin Dynamics simulations with stochastic noise term to study global relaxation time for topologically modified bead-spring models of polymer chain. The center of each monomer is connected by spring of spring constant κ to the center of adjacent neighboring monomers; i.e. two adjacent monomers interact via Harmonic potential. The equilibrium length of the spring connecting the two monomers is denoted by a. Additionally, all the monomers of the polymer interact with each other via Weeks-Chandler-Anderson (WCA) potential given by:

$$\Phi_{\mathrm{WCA}}(r) = \begin{cases} 4\epsilon\left[\left(\frac{\sigma}{r}\right)^{12} - \left(\frac{\sigma}{r}\right)^{6}\right] + \epsilon & \text{if } r < 2^{1/6}\sigma, \\ 0 & \text{if } r \geq 2^{1/6}\sigma. \end{cases}$$

Here σ is the diameter of the monomers and r is the radial distance between center of two monomers. The WCA interaction is repulsive in nature and prevents monomers from coming very close to each other. The harmonic potential energy of the spring is then given by $\kappa(r-a)^2$, where $kappa = 100\frac{K_B T}{a^2}$. Here K_B is the Boltzmann constant and T is the temperature of the system.

Since we are working in melt conditions with non-entangled and relatively short polymers i.e. the Rouse Modes regime, the topological constraints due to presence of many other polymers do not play a dominant role. The presence of other chains can simply be incorporated by using a stochastic noise background. Thus, we investigate the dynamics of our topologically modified polymers using the Langevin Dynamics simulations with stochastic noise term. As the length of polymer increases one can no longer accurately study the dynamics using simple Langevin dynamics because now the entanglement effects starts to dominate. This is known as the Reptation regime. In this thesis, we do not deal with long polymer chains which adds more complexity to the problem and hence we can use Langevin equation for our model system.

The Langevin equation is as follows:

$$m\frac{d^2\vec{r}}{dt^2} = -\gamma\frac{d\vec{r}}{dt} + f_{\text{ext}} + \eta(t) \tag{2.2}$$

Here $\eta(t)$ is the time-dependent Gaussian stochastic noise term, γ is the damping coefficient,m denotes particle mass and f_{ext} represents external force on the system. For our case external force is absent. The noise term with Gaussian probability distribution has some properties as follows:

$$\langle \eta(t) \rangle = 0 \tag{2.3}$$

$$\langle \eta_i(t)\eta_j(t') \rangle = 2\gamma k_B T\, \delta_{i,j}\delta(t-t') \tag{2.4}$$

There are multiple informative points that can be inferred from equation 2.4. Firstly, it tells us how the stochastic noise term is related to damping coefficient, which can further be written in terms of diffusion constant using Stokes-Einstein relation. Secondly, it states that Gaussian white noise is proportional to temperature or the thermal energy of the system. Third it also tells us that the noise is uncorrelated over time.

2.3 Algorithm Details

Before performing Langevin Dynamics (LD) simulation we first perform Monte Carlo (MC) simulation for $2 * 10^3$ iterations. This helps to randomize the initial conditions, for example, by randomizing initial position of monomers across the ensemble of runs we are doing. And it also lowers down the energy of the system before the Langevin Dynamics simulations begins.

The Monte Carlo (MC) algorithm is as follows:

Algorithm 1 Monte Carlo Simulation for Monomer Displacement

Initialize the system with N monomers
for each Monte Carlo step (MCS) from 1 to 2000 **do**
  for each monomer $i = 1$ to N **do**
    Generate a trial displacement in a random direction
    Compute the energy change ΔE
    if $\Delta E < 0$ **then**
      Accept the displacement
    else
      Accept the displacement with probability $e^{-\Delta E/k_B T}$
    end if
  end for
end for=0

Then we perform the Langevin Dynamics simulation which follows the following algorithm:

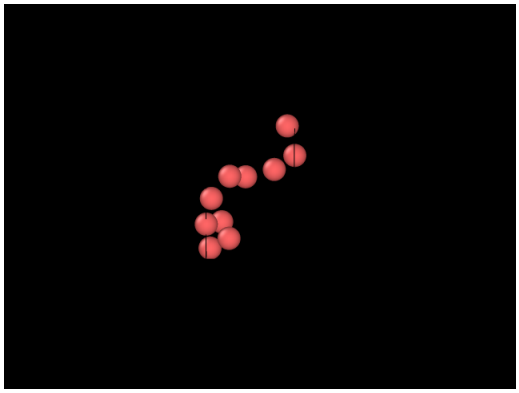

Figure 2.2: The figure represents snapshot of LD simulation of Linear Polymer chain with 10 monomers.

The a_i term in the algorithm below denotes the acceleration of the i_{th} particle. The way the algorithm works is it updates the position of the particle, then it updates the force on each monomer based on the updated position. Then it updates the velocity of the particle which is dependent on both the new force and the force at the previous timestep. We run the simulation for 1.5 million timesteps first to let the system equilibrate. The we run it further for $2 * 10^8$ iterations and collect the relevant statistical data. For all the case studies

Algorithm 2 Langevin Dynamics Simulation using Velocity Verlet

Initialize positions $\{r_i\}$ and velocities $\{v_i\}$ for all monomers
Set temperature T and friction coefficient γ
Run equilibration for 1.5×10^6 steps (no data collection)
for each step from 1 to 2×10^8 **do**
  for each monomer i **do**
    Compute new position:

$$r_i(t + \Delta t) = r_i(t) + v_i(t)\Delta t + \frac{1}{2}a_i(t)(\Delta t)^2$$

  end for
  Compute forces on each monomer (spring force + WCA potential)
  for each monomer i **do**
    Compute new velocity:

$$v_i(t + \Delta t) = v_i(t) + \frac{1}{2}(a_i(t) + a_i(t + \Delta t))\Delta t$$

    Add stochastic Gaussian noise term:

$$v_i(t + \Delta t) \leftarrow v_i(t + \Delta t) - \frac{\gamma}{m}v_i(t)\Delta t + \text{Noise}$$

  end for
  if step $\geq 1.5 \times 10^6$ **then**
    Collect statistical data
  end if
end for
=0

that we will mention in the future chapters, we have carried 20 independent runs for each system with each for $2 * 10^8$ iterations. Then we do analysis for the data we have obtained to make inferences based on the results. We have applied Periodic Boundary Conditions with Center of Mass of the polymer recentered at every timestep.

2.3.1 LAMMPS Simulation Parameters

- Units = LJ
- Atom style = angle
- Boundary = Periodic
- K_BT (Temperature) = 1
- κ (Spring Constant) = 100
- a (equilibrium spring length) = 1.0
- γ(damping coefficient) = 1.0
- σ (diameter of each monomer) = 0.8
- ϵ =1.0
- LJ potential cutoff = 0.898 LJ units
- Δt (simulation timestep) = 0.01

2.4 Modified Polymer Topologies used

In this thesis we have worked with many topologically modified polymer topologies. Here I will describe all of them as a reference for further chapters. We have polymers with length ranging from 100 to 500 for all of them but the figures drawn below are assumed to have total number of monomers to be 100. The monomers cross-linked to each other to create complex topologies change appropriately as the total number of monomers increases. The

modified topologies that we mainly focus on are shown in the figure below. In the subsequent sections we talk about structural details of these topologies and further modifications.

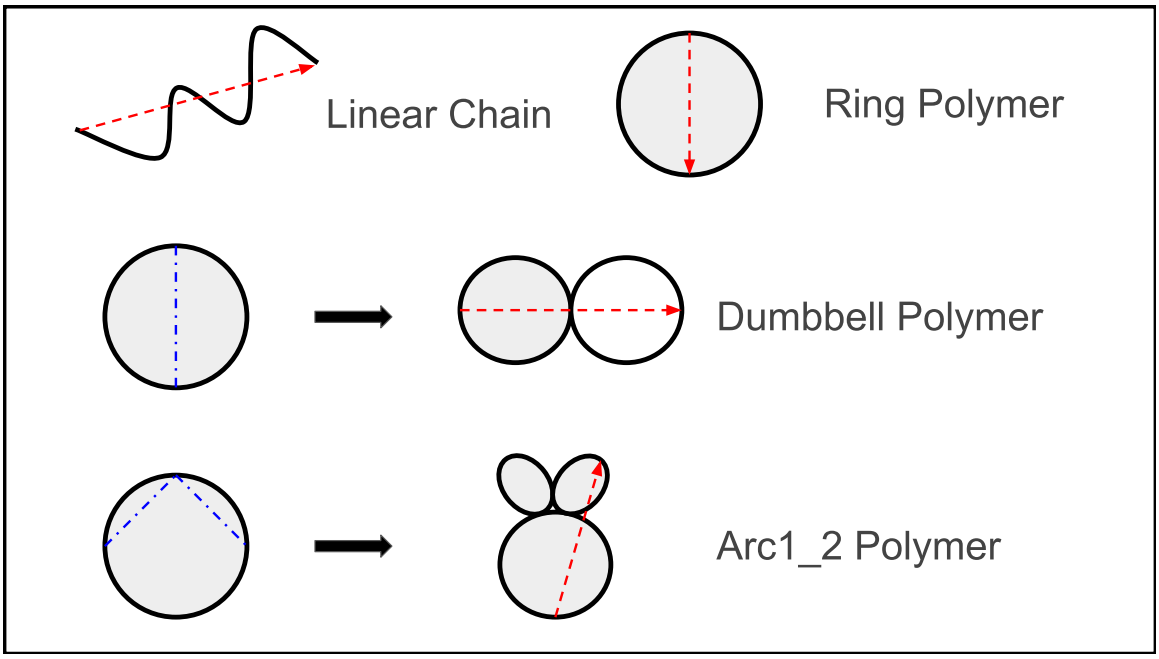

Figure 2.3: Schematics of Topologically Modified Polymer. The subsequent sections explain the structural details of these topological polymers.

2.4.1 Linear Polymer

The simplest polymer topology is the linear polymer chain with two free ends. The red arrow represents the end-to-end vector we will study in the next chapter.

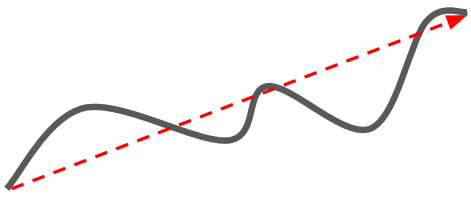

Figure 2.4: Linear Polymer chain.

2.4.2 Ring Polymer

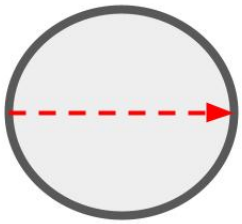

Figure 2.5: Ring Polymer.

A ring polymer is simply formed by joining two free ends of a linear polymer chain. Here the red dotted arrow is a diametric vector and since all the diametric vectors are identical one can choose any diametric vector for analysis purposes.

2.4.3 Dumbbell/Inverted-8 Polymer

A dumbbell polymer is made by adding one additional crosslink between two non-adjacent monomers on a ring. This will lead two formation of two loops. We work with different ratios of loops in case of Dumbbell, each is described below.

Symmetric Dumbbell

In case of Symmetric Dumbbell, we join two diametrically opposite monomers on a ring polymer. This leads to two identically sized loops, for example, if we have 100 monomers in total then each loop will contain 50 monomers. In the figure below the red vector spans both the loops and it is the longest vector. We also have two additional vectors inside one loop, the green vector is placed at some distance away from cross-link whereas the blue vector has one end on the cross-link.

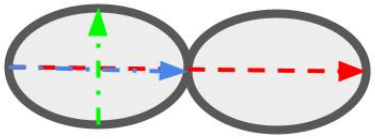

Figure 2.6: Symmetric Dumbbell Polymer.

Dumbbell 10%

Here 10% means that one loop (smaller loop) contains 10% of total monomers in the polymer. So for case of 100 total monomers, small loop will contain 10 monomers and the bigger loop

will contain 90 monomers. In this case as you can see below in the figure, the cross link is added between the 5th and 95th monomer.

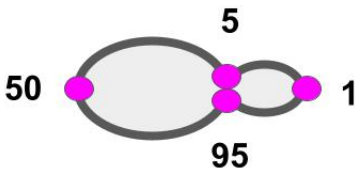

Figure 2.7: Dumbbell 10% Polymer.

Other ratios of Dumbbell Polymers

Apart from 10% we have studied three other ratios of dumbbell polymers, those being - 20%, 25%, 30%. In each of these cases the percentages convey the amount of polymers in the small loop as above. Let's say, if we take an example of Dumbbell 20% polymer with total 100 monomers, then the small loop will contain 20 monomers. This can be done by creating an additional cross link between the 10th and 90th monomer in a ring polymer of 100 monomers. The same logic applies for other ratios as well. Here crosslinks mean connecting them by harmonic spring.

2.4.4 Arc1_2 Polymer

Similar to the case of Dumbbell polymers, here too we work with different ratios of loops. Now Arc1_2 architecture has three loops, out of which two loops are identical in size. This topology can be achieved by adding two crosslinks in the ring polymer. The figure below can be seen to understand it better.

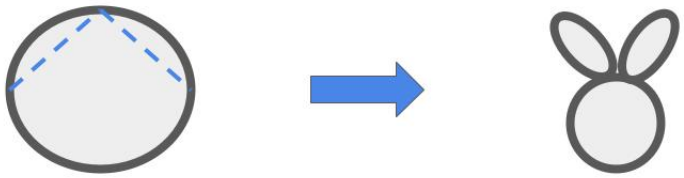

Figure 2.8: Arc1_2 Formation.

Symmetric Arc1_2 Polymer

Let us define a ratio:

$$r = \frac{\sum \text{Monomers in two identical loops}}{\text{Monomers in third loop}} \tag{2.5}$$

Now in case of symmetric Arc1_2 polymer, the ratio r is equal to 1. This means the sum of monomers in two identical loops is equal to the monomers in third loop. So for example, if we have 100 monomers in total, two identical loops will have 25 monomers each and the third loop will have 50 monomers. The figure is shown below :

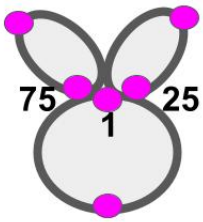

Figure 2.9: Symmetric Arc1_2 polymer.

Arc1_2 90% Polymer

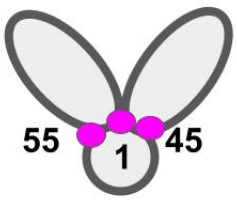

Figure 2.10: Arc1_2 90% polymer.

Here 90% just means the ratio(r)*100. So if there are 100 monomers in total, ratio of 0.9 would mean sum of monomers in two identical loops is 90 with each having 45 monomers and

the third loop will have 10 monomers. In the figure above you can see the visual description of how it would look like. This can be achieved by creating a cross-link between 1st and 45th monomer, and 1st and 55th monomer of a ring polymer.

Other ratios of Arc1_2 Polymers

Here too we have worked with different ratios, particularly - 10%, 30%, 70%, and 90%. Arc1_2 with 90% ratio was illustrated on the previous page. Similarly, other ratios can also be imagined. One thing to note here is that for ratios of 10% and 30% the two identically sized loops are smaller than the third loop, whereas for 70% they are slightly larger than third loop (almost equally sized) and for 90% they are significantly larger than the third loop.

2.4.5 Other modified Topologies

We have also worked with some other modified topologies which can be seen in the below figures:

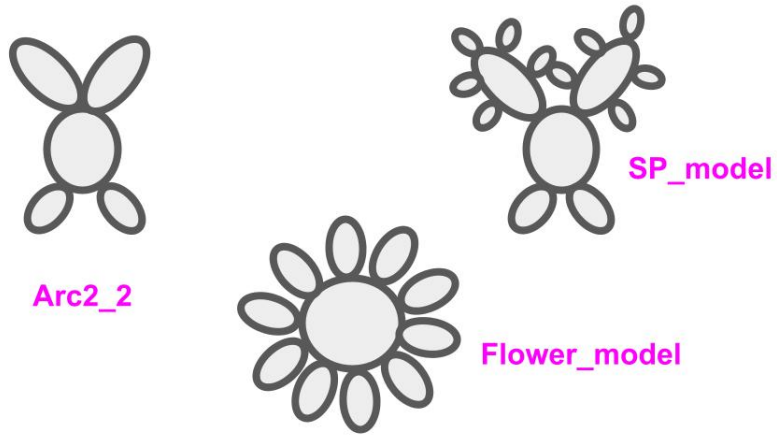

Figure 2.11: The left figure shows Arc2_2 polymer, bottom center is the Flower model, and the right figure is the SP_model.

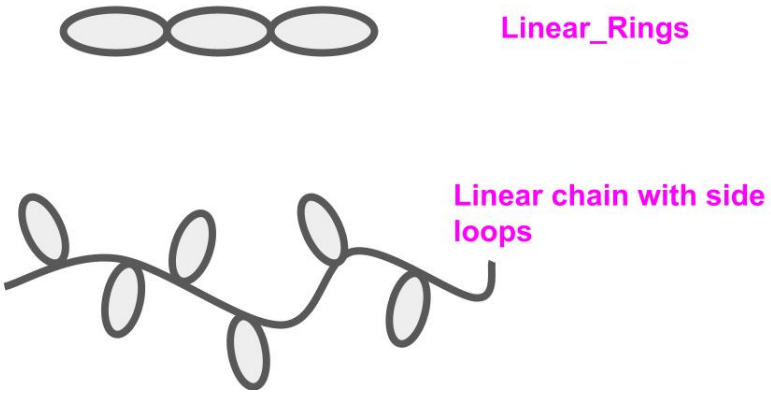

Figure 2.12: The top figure shows linearly attached rings model and the bottom figure shows linear chain with side loops model

2.4.6 Semiflexible Polymer Chain

In the case of semi-flexible linear chain, we take into account three-body interactions between any three consecutive monomers. The two bonds between three consecutive adjacent monomers using the harmonic interaction give by following:

$$V_\theta = \frac{\kappa \left(\theta - \theta_0\right)^2}{2} \tag{2.6}$$

Here κ is the associated bending energy constant and θ_0 is the equilibrium bond angle of 180 degrees.

Chapter 3

Relaxation of End-to-End Vectors

3.1 Theory and Algorithm

3.1.1 Rouse Model

Rouse model is considered to be the first successful molecular model of polymer dynamics named after Rouse who developed the model. Let's say there are N beads connected by spring of root-mean-square size b and the friction coefficient of each bead is given by ζ. This means the total friction constant for the polymer chain with N beads is $\zeta_R = N\zeta$. The viscous frictional force on the chain is given by $\vec{f} = -N\zeta\vec{v}$, where $\vec{v}$ is the velocity with which the chain is being pulled. Using Einstein's relation, the diffusion constant of Rouse chain is given as:

$$D_R = \frac{kT}{\zeta_R} = \frac{kT}{N\zeta} \tag{3.1}$$

Rouse Time is defined as the time a polymer chain takes to diffuse a distance of the order of its size and it is given by:

$$\tau_R \approx \frac{R^2}{D_R} \approx \frac{R^2}{\frac{kT}{N\zeta}} = \frac{\zeta}{kT} N R^2 \tag{3.2}$$

The Rouse time has a property that at timescale shorter than Rouse time the system exhibits viscoelastic modes, however, at larger timescale the dynamics is simply diffusive.
The size of a polymer chain is related to the number of monomers by a power law:

$$R \approx bN^{\nu} \tag{3.3}$$

For ideal linear chain, $\nu = 0.5$ and for real linear chain $\nu = 0.6$. The Rouse time of ideal linear chain is given by the product of individual beads relaxation time, known as **Kuhn monomer relaxation time**:

$$\tau_0 \approx \frac{\zeta b^2}{kT} \tag{3.4}$$

Using equation 3.2 and equation 3.3 we can write:

$$\tau_R \approx \frac{\zeta}{kT} N R^2 = \frac{\zeta b^2}{kT} N^{1+2\nu} \approx \tau_0 N^{1+2\nu} \tag{3.5}$$

The exact relation can be calculated and is given as:

$$\tau_R = \frac{\zeta b^2}{6\pi^2 kT} N^2 \tag{3.6}$$

This is known as **Rouse stress relaxation time**, Rouse end-to-end vector relaxation time is double of the above time and is given by:

$$\tau = \frac{\zeta b^2}{3\pi^2 kT} N^2 \tag{3.7}$$

In Rouse Model, the longest relaxation time of an ideal polymer chain is $\tau_R \approx \tau_0 N^2$ but there also exists modes of relaxation. For example, pth mode of relaxation deals with relaxation at scales of $\frac{N}{p}$ monomers. The relaxation time of pth mode is given by:

$$\tau_p \approx \tau_0 \left(\frac{N}{p}\right)^2 \tag{3.8}$$

3.1.2 Algorithm

For end-to-end vector relaxation the algorithm we use is as follows:

Algorithm 3 End-to-end vector Time Autocorrelation

Initialize $N_{\text{steps}} \leftarrow 2 \times 10^8$ (total timesteps)
Initialize $M \leftarrow 20$ (number of independent runs)
for $i \leftarrow 1$ to M **do**
    Load vector data $\vec{v}(t)$ for $t = 1$ to N_{steps} from LAMMPS
    for $dt \leftarrow 1$ to N_{steps} **do**
        for $t \leftarrow 1$ to $N_{\text{steps}} - dt$ **do**
            Compute autocorrelation: $\dot{A}_i(dt) = \vec{v}(t + dt) \cdot \vec{v}(t)$
        end for
        Store $\dot{A}_i(dt)$ for all t in file i
    end for
end for
Initialize average autocorrelation $\dot{A}_{\text{avg}}(dt) \leftarrow 0$
for $dt \leftarrow 1$ to N_{steps} **do**
    Compute average: $\dot{A}_{\text{avg}}(dt) = \frac{1}{M} \sum_{i=1}^{M} \dot{A}_i(dt)$
end for
Store $\dot{A}_{\text{avg}}(dt)$ as the final result in a file =0

We perform the time autocorrelation of vector data between two monomers. This has been done for 20 independent runs and then for analysis we take the average over this 20 runs to

get well-averaged results and avoid any specificity to one initial condition.

3.2 Results

For all the cases below, while fitting the vector time autocorrelation data during analysis, we fit the first three odd rouse modes instead of just the first rouse mode to get better accuracy for the relaxation time. The vector time autocorrelation is a decaying graph which we fit with the following function:

$$y = a\left[\exp(-(x/b)) + \frac{1}{9}(\exp(-9(x/b)) + \frac{1}{25}(\exp(-25(x/b))\right] \tag{3.9}$$

where a is normalizing constant and b is the relaxation time.

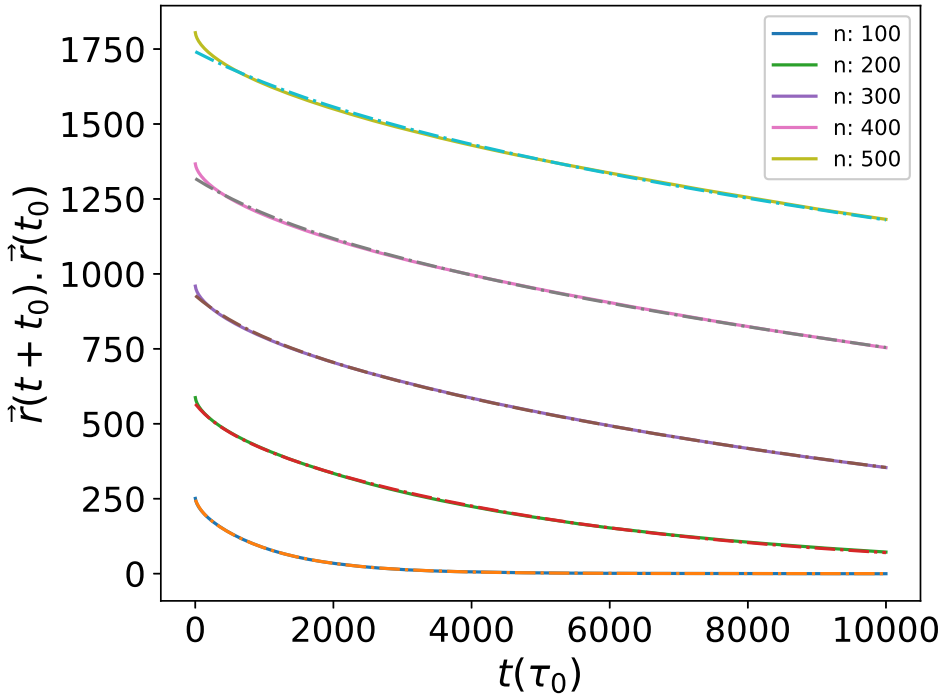

Figure 3.1: The graph shows end-to-end vector relaxation of linear chain. The dotted line represents the first three odd rouse modes fitting function we use to obtain the relaxation time.

For the case of Linear Polymer, end-to-end vector is simply the vector connecting the two monomers at free ends of the chain. As you can see from the figure 3.2, the relaxation time for polymer with larger number of monomers take more time to relax as compared to linear chains with lower number of monomers. The decaying graph represents the timescales at which the polymer changes its conformation. The relaxation time obtained follows a scaling relation of $\tau \propto N^{2.2}$ for linear chains with excluded volume interaction as suggested by theory. We also observe similar scaling for vectors in ring polymer and dumbbell polymer. For ring polymer an end-to-end vector does not exist, so we choose any one of the diametric vectors to do the analysis. For dumbbell architecture, it is not clear which vector to choose, but the data we represent here corresponds to the red vector shown in the schematic of dumbbell architecture in the previous chapter. We can see linear takes the most amount of time to relax whereas ring takes the least for the same number of monomers.

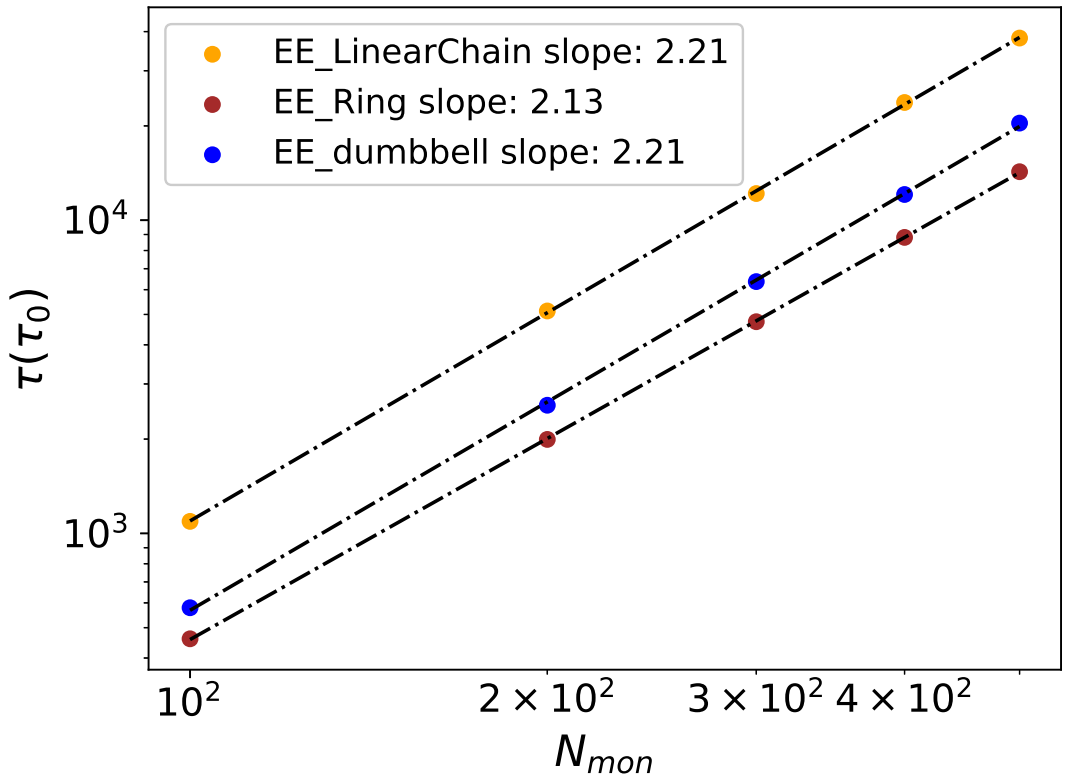

Figure 3.2: The graph shows scaling of End-to-End vector relaxation time with number of monomers for linear polymer, ring polymer and dumbbell polymer. They follow a scaling of $\tau \propto N^{2.2}$.

Dumbbell Polymer

The schematics of dumbbell is shown again below:

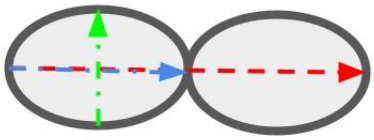

Figure 3.3: The schematic of dumbbell polymer.

Now in the above figure we also investigate thee relaxation dynamics of green and blue vectors. The blue vector has one end on the cross-link whereas the green vector has both the ends away from cross-link. By investigating the relaxation dynamics of this two vectors we can get insights into the effect of crosslink on relaxation time.
In the graph below, the EE_crosslink_vector corresponds to the blue vector and EE_diametric _vector corresponds to the green vector. From the graph we can infer that the vector passing through the crosslink takes more time to relax than the other vector. We can also see that the relaxation time increases for both vectors as the polymer size increases and consequently the size of vectors as well. The difference between relaxation time between both vectors is more pronounced for larger polymers because in addition to cross link now the size difference is also more for the case of larger polymers.

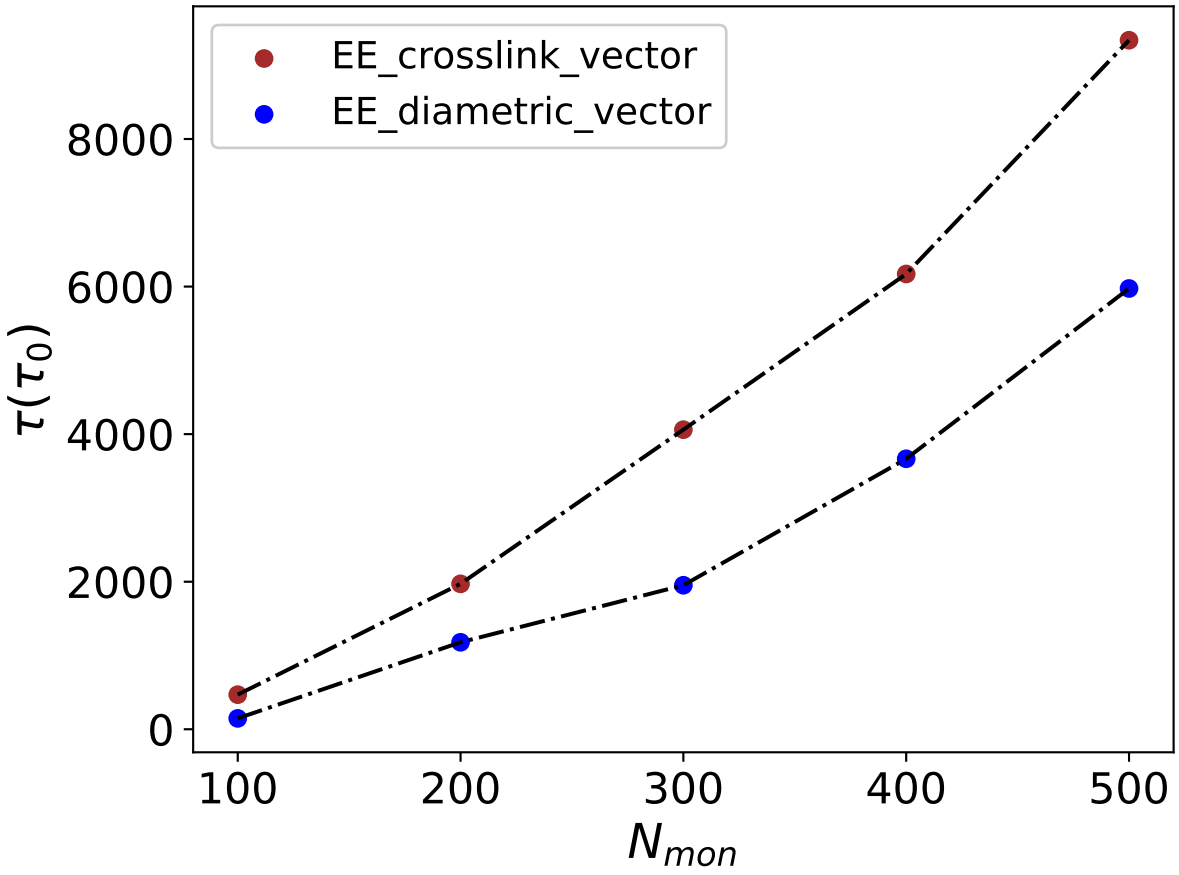

Figure 3.4: The relaxation time of vectors in dumbbell subloop. It shows that vector connected to the crosslink takes longer time to relax than a diametric vector in the subloop not passing through the crosslink

3.2.1 Problems with End-to-End vector Relaxation method

The problem with studying relaxation of end-to-end vectors is that it is not well defined apart from linear polymers. In case of ring polymer one can choose any diametric vector since all of them are identical. But once you get to more complex topologies, choosing vectors becomes very ambiguous with no clear reason to prefer one vector over another. One of the examples of this ambiguity can be seen in the figure below, Here all the three red, green and pink vectors are roughly of equal size but there is not clear reason to choose one over another. Similarly when we move to more complicated topologies like Arc1_2 for example, the options

to select vectors from grows exponentially. Hence, we see a need for more general method to characterize relaxation time of topologically modified polymers which is independent of size and internal structural details of polymer architectures.

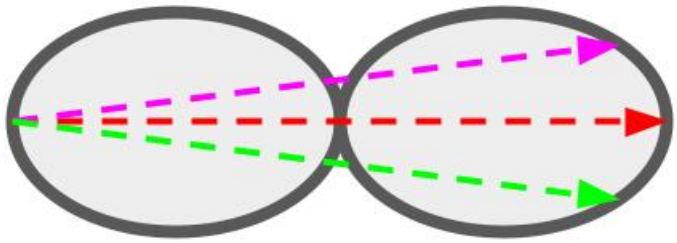

Figure 3.5: The schematic shows three vectors for symmetric dumbbell polymer to represent ambiguity in choosing vectors.

Chapter 4

Relaxation of correlation in fluctuations of Radius of Gyration (C_g)

4.1 Theory and Algorithm

4.1.1 Method Description

In the previous chapter, we have seen the shortcomings of using end-to-end vectors in studying the relaxation time of a polymer. Those were mainly the dependence of that method on the internal topological details of the polymer and secondly it also depended on the length of the vector whose choice was very ambiguous. Hence in this chapter we study the global relaxation time using a general method which overcomes these issues from the previous method. We determine the global relaxation time τ by exponentially fitting the decaying autocorrelation function given by:

$$C_g(t) = \frac{\langle (R_g(t+dt) - \langle R_g \rangle)\,(R_g(t) - \langle R_g \rangle) \rangle}{\left\langle R_g^2 \right\rangle - \langle R_g \rangle^2} \tag{4.1}$$

We fit the decaying function above by the slowest exponential decay of the form $C_g(t) = e^{-\frac{t}{\tau_g}}$, where τ_g is the global relaxation time. Since the $C_g(t)$ term is normalized by the variance of R_g, irrespective of the length of the polymer chain, the $C_g(t)$ term will always start from 1.0. Hence while fitting with exponential function the prefactor is just 1.0. This $C_g(t)$ term measures correlation in fluctuations of radius of gyration about its mean value.

Here R_g is the radius of gyration defined as :

$$R_g^2 = \frac{1}{N}\sum_{i=1}^{N}\left(\vec{R_i} - \vec{R_{cm}}\right)^2 \tag{4.2}$$

$$\vec{R_{cm}} = \frac{1}{N}\sum_{j=1}^{N}\vec{R_j} \tag{4.3}$$

One thing to note here is that even though the relaxation time means the equilibration time of the system, here it does not tell you how much time it takes for the polymer to come to equilibrium in the simulation. Instead, here we have already minimized the energy of the system using Monte Carlo fix and additionally we also run the Langevin Dynamics simulation for 1.5×10^6 iterations to let the system achieve equilibrium. So what does looking relaxation time mean here? It tells us that if we make an observation about the state of the system at any arbitrary time t_0, after how long we will reach a state where we won't be able to tell what initial state or conditions we started with. In a sense, relaxation time here is telling us the timescale at which the polymer modifies its configuration. Hence, it is interesting and relevant to look at how topological modifications in these ring polymeric systems affect this timescale from both polymer physics and biological standpoint. Hence, the next two chapters will be a systematic investigation of relation between topological modifications and the relaxation time of those polymers.

4.1.2 Algorithm

Algorithm 4 Calculation of Correlation Function $C_g(dt)$

Initialize Parameters:
Run Monte Carlo fix to minimize energy and randomize initial conditions
Set total simulation time $T = 2 \times 10^8$ iterations
Set number of independent runs $N_{\text{runs}} = 20$
for $i = 1$ to N_{runs} **do** {Loop over independent runs}
  Compute Radius of Gyration R_g
  Run LAMMPS Langevin Dynamics simulation for 1.5×10^6 iterations to let system equilibriate
  Run LAMMPS Langevin Dynamics simulation to obtain $R_g(t)$ at each timestep t
  Compute time-averaged R_g over all T iterations:
  $\langle R_g \rangle = \frac{1}{T} \sum_{t=1}^{T} R_g(t)$
  Compute Correlation $C_g(dt)$
  for $dt = 1$ to T **do** {Loop over time differences}
    for $t = 1, T - dt$ **do**
      Compute $C_g(dt)$ using:
      $C_g(t) = \frac{\langle (R_g(t+dt) - \langle R_g \rangle)(R_g(t) - \langle R_g \rangle) \rangle}{\langle R_g^2 \rangle - \langle R_g \rangle^2}$
    end for
  end for
end for
Compute Average $C_g(dt)$ **Over All Runs:**
for $dt = 1$ to T **do**
  Compute final averaged correlation:
  $\langle C_g(dt) \rangle = \frac{1}{N_{\text{runs}}} \sum_{i=1}^{N_{\text{runs}}} C_g^i(dt)$
end for=0

4.2 Linear Polymer, Ring Polymer and Symmetric Dumbbell Polymer

As we stated in the previous subsection that C_g is the decaying correlation function that we fit with an exponential function to get the relaxation time. Here in the figure below I have plotted this function for the case of Linear Polymer.

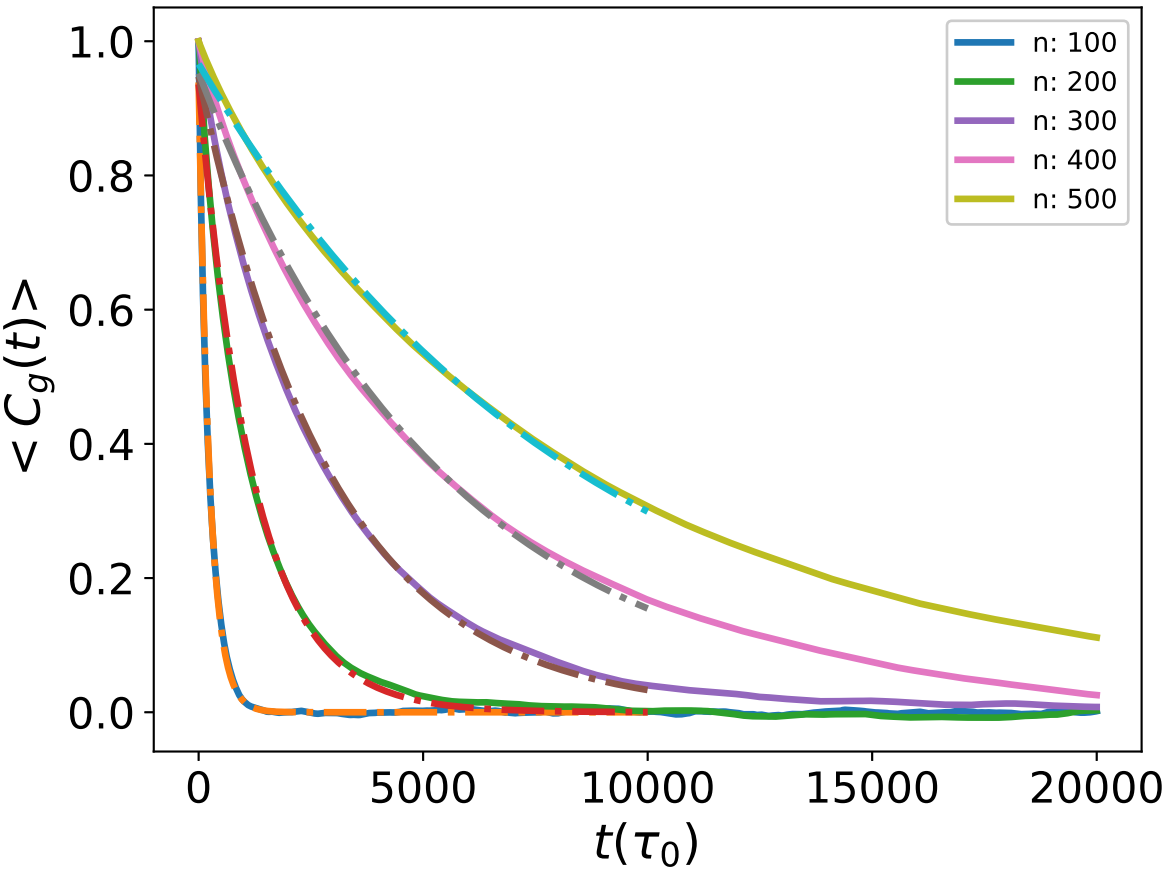

Figure 4.1: The graph shows decaying correlation function C_g as a function of time for different lengths of Linear Polymer Chain.

The figure 4.1 represents the decaying C_g graph for Linear Polymer chain with varying chain length; specifically number of monomers here are 100, 200, 300, 400, and 500. The dotted line represents the exponential fitting we are fitting with and the solid line represents the data generated from the simulation. We observe here that similar to the case of end-to-end

vectors case the $\langle C_g(t) \rangle$ takes more time to decay to zero as the chain length increases. Now in order to extract the relaxation time from the exponential we need to take the linear range of the data. This is because we are fitting the graph with $C_g(t) = e^{-\frac{t}{\tau_g}}$. Now taking logarithm on both the sides:

$$log(C_g(t)) = -\frac{t}{\tau_g} \tag{4.4}$$

So plotting the semi-log graph with $log(C_g(t)$ on the y-axis and time on the x-axis, we should get a linear line whose inverse of slope can give us the relaxation time. So when we plot this semi-log plot, we look for this linear line regime and extract the slope of the linear line to find out the relaxation time. This has been explicitly shown in the figure 4.2 below.

In figure 4.2 [a] we see the semi-log plot for two linear polymer chains of length 400 and 500 monomers. The orange dotted line represents the linear range of data we use to fit the exponential and extract the relaxation time from the slope. One can clearly see that we cannot use entire range of our data here because it is not linear at all times.
In figure 4.2 [b] we see the scaling relation between relaxation time and number of monomers for linear polymer chain of length 100 to 1000 monomers range. And similar to end-to-end vector scaling relation theory, here too we see a scaling of:

$$\tau_g \propto N^{2.2} \tag{4.5}$$

This is interesting because now we are not using a structurally dependent quantity like end-to-end vectors, instead, we have turned towards a more general or globalized quantity i.e. correlations in fluctuations of Radius of Gyration R_g and R_g is a general measure which is unambiguously measurable for any topologically modified polymers. Over this basic study for linear polymer chain, we use this relaxation of C_g method for more complex topologies.

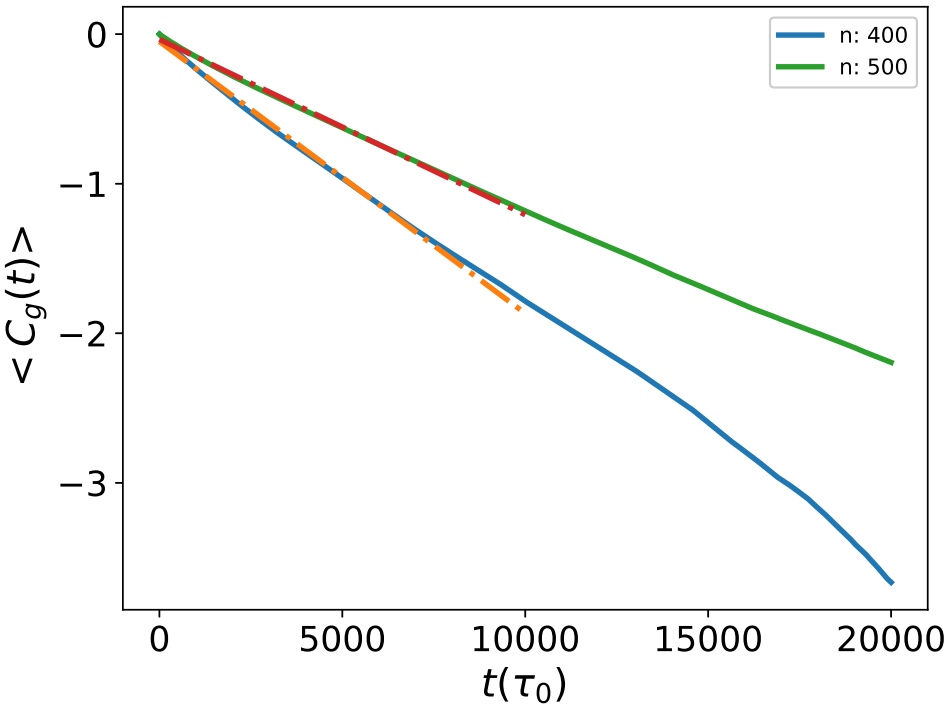

[a]

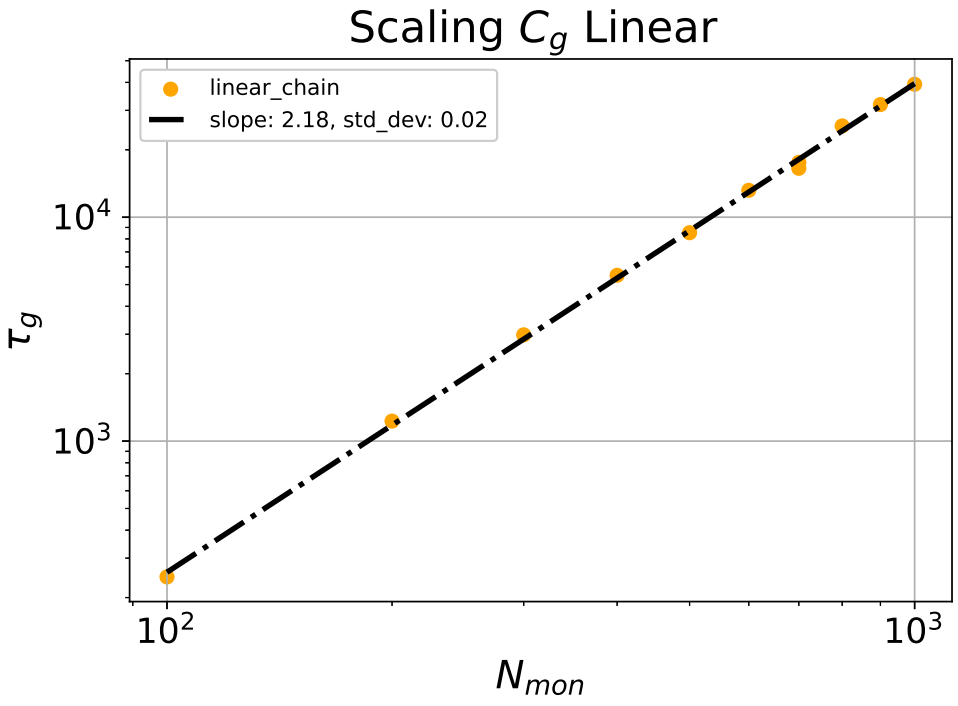

[b]

Figure 4.2: Figure a shows semi-log plot for C_g relaxation time and the dotted line shows the range of data we use to extract relaxation time. Figure b shows scaling between C_g relaxation time and Number of monomers for linear chain, it follows $\tau_g \propto N^{2.2}$

Now in the figure below we compare the scaling relations for Linear Polymer, Ring Polymer, Symmetric Dumbbell polymer, and Symmetric Arc1_2 Polymer.

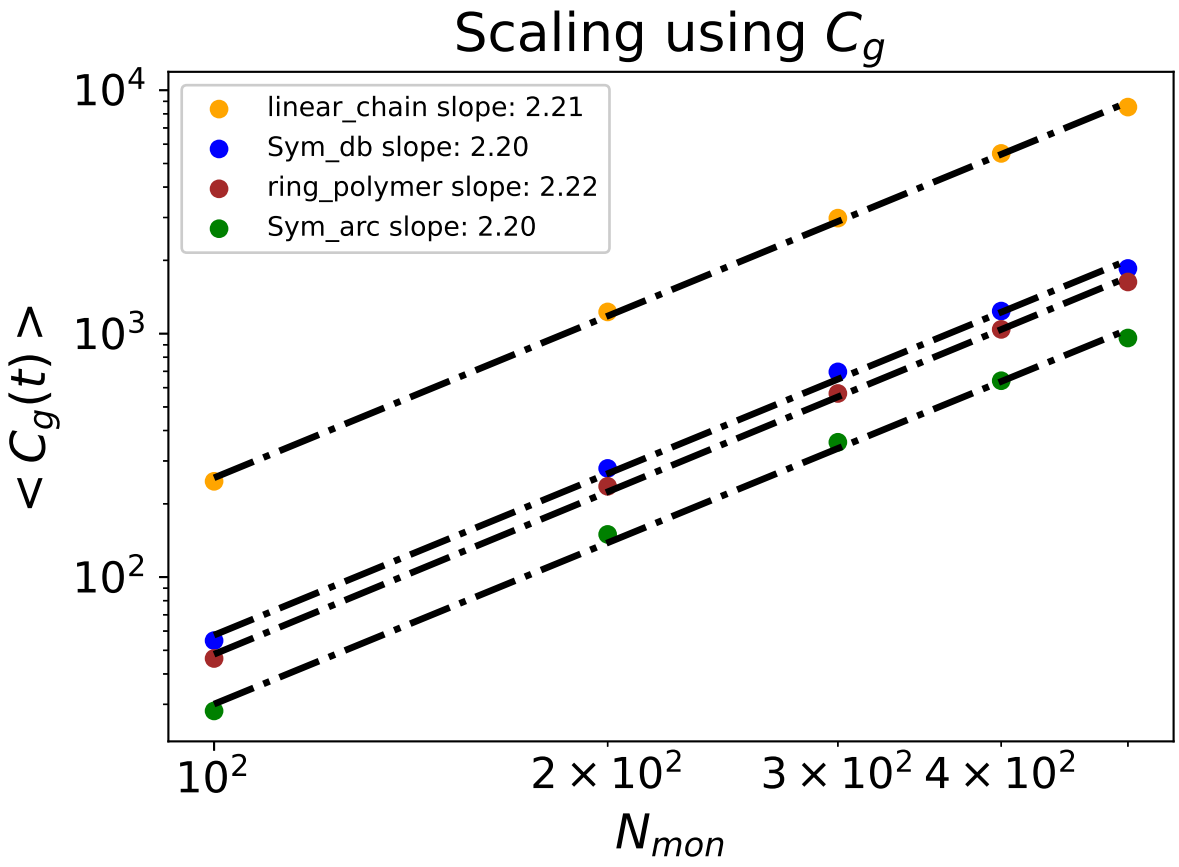

Figure 4.3: The graph shows scaling of C_g relaxation time for Linear Polymer, Ring Polymer, Dumbbell Polymer and Symmetric Arc_2 polymer with the total number of monomers.

We observe from the graph that all topologies, specifically, linear chain, ring, symmetric dumbbell, and arc1_2 polymers, follow the same scaling relation of $\tau_g \propto N^{2.2}$. We do not take into consideration the second decimal place value due to statistical error since we only have data values for the case of polymer length from 100 to 500 total monomers. We have not used too high values of polymer length because it is computationally very expensive, both in terms of storage and time. One can notice that we get the same order of time taken to relax among different topologies as we obtained using the end-to-end vector relaxation method. We saw there as well that the Linear polymer chain took the highest time, the

Symmetric Dumbbell was in the middle, and the Ring Polymer took lesser time than both Linear and Ring. Here too we see the same trend with symmetric Arc1_2 polymer taking even less time to relax than the ring polymer. So despite of the shortcomings in the End-to-End vector method, we do get some idea of trend between different topologies. Furthermore, the same trend using this method validates our results and gives confidence in the C_g relaxation method to do more deep analysis using it. So, a conclusive point here is:

Linear Polymer > Symmetric Dumbbell > Ring Polymer > Symmetric Arc1_2

4.3 Asymmetric Dumbbell Polymers

Using the same C_g relaxation method we analyze the dynamics of asymmetric dumbbell polymer architectures. This asymmetry arises because unlike the above symmetric case where both the loops of the dumbbell polymer had same number of monomers, here the number of monomers in both the loops are different. We systematically study the relation between these unequal loop sizes and their to the relaxation time of the polymer. In the figure 4.4 below we can see the scaling relation graph for different ratios of dumbbell. The y-axis is the Relaxation time and x-axis is the number of monomers and the graph is drawn in logarithmic scale. This gives the scaling relation.

In figure 4.5 the plot between relaxation time and monomers where we see the relaxation time increases with number of monomers. Here we see that Dumbbell with ratio 1:9 takes lesser time to relax compared to ring polymer of the same length. But Dumbbell with ratio 3:7 takes more time than the ring polymer as similar to the symmetric Dumbbell case.

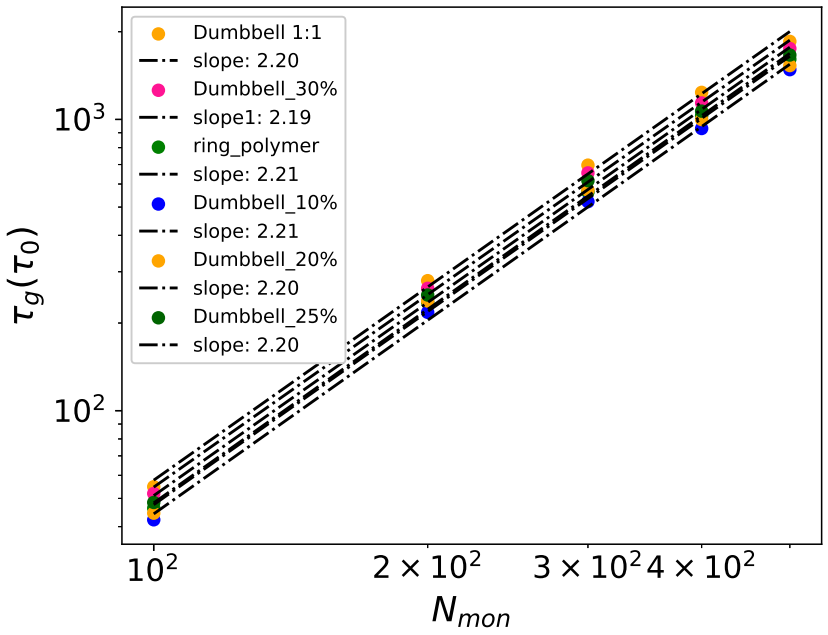

Figure 4.4: The graph shows scaling of $\tau_g \propto N^{2.2}$ for Symmetric Dumbbell, Dumbbell of ratios 10%, 20%, 25%, and 30% with the total number of monomers.

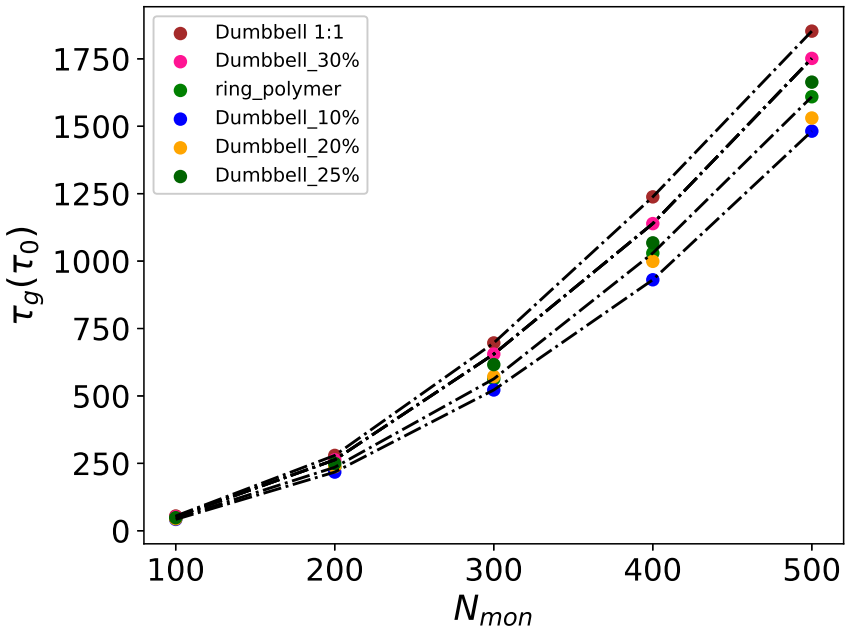

Figure 4.5: The graph shows C_g relaxation time for Symmetric Dumbbell, Dumbbell of ratios 10%, 20%, 25%, and 30% with the total number of monomers.

In the figure 4.6 below represents a plot of relaxation time against ratios graph for different dumbbell architectures for the case of total 500 monomers. The ratio basically is Monomers in small loop divided by monomers in the big loop. So ratio 0 indicates no small loop or essentially just a ring polymer. Similarly, ratio of 1 indicates a symmetric Dumbbell polymer.

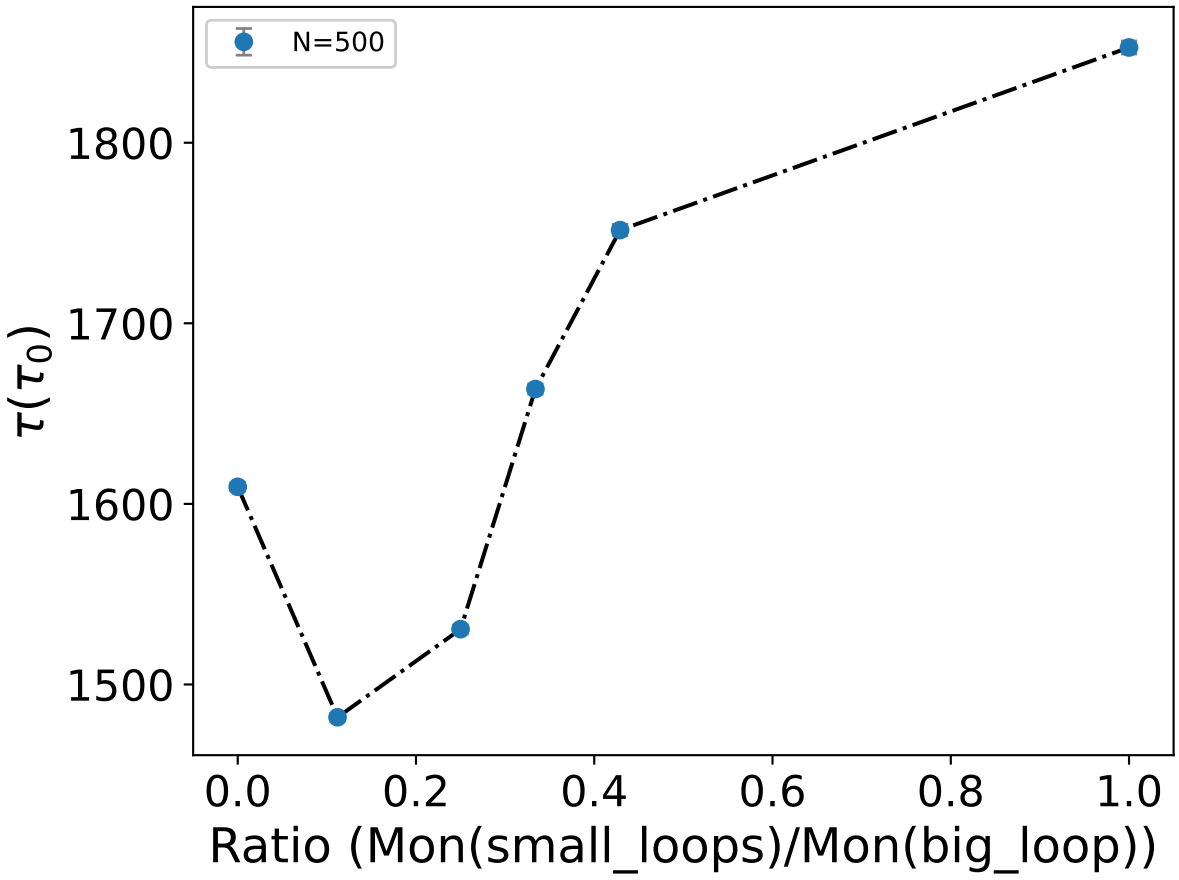

Figure 4.6: The graph shows C_g relaxation time for Symmetric Dumbbell, Dumbbell of ratios 10%, 20%, 25%, and 30% with the total number of monomers equal to 500.

Here we saw an interesting property that certain dumbbell ratios show faster relaxation dynamics, a non-monotonous behavior, than ring contradictory to the expectation that relaxation time would show a monotonous decrease towards ring. The next sections will be towards re-validating these results and then working towards explaining this non-monotonous behavior of relaxation dynamics.

Symmetric Dumbbell > Dumbbell 3:7 > Dumbbell 1:3 > Ring Polymer > Dumbbell 1:4 > Dumbbell 1:9

4.4 Asymmetric Arc1_2 Polymers

We have done similar investigation with different ratios of Arc1_2 polymers. Here ratio,r, is:

$$r = \frac{\sum(N_{mon} \text{ two identical loops})}{N_{mon}\text{third loop}} \tag{4.6}$$

In the figure 4.7 below you can see the scaling relation between different Arc1_2 polymer ratios against number of monomers on the logarithmic scale.

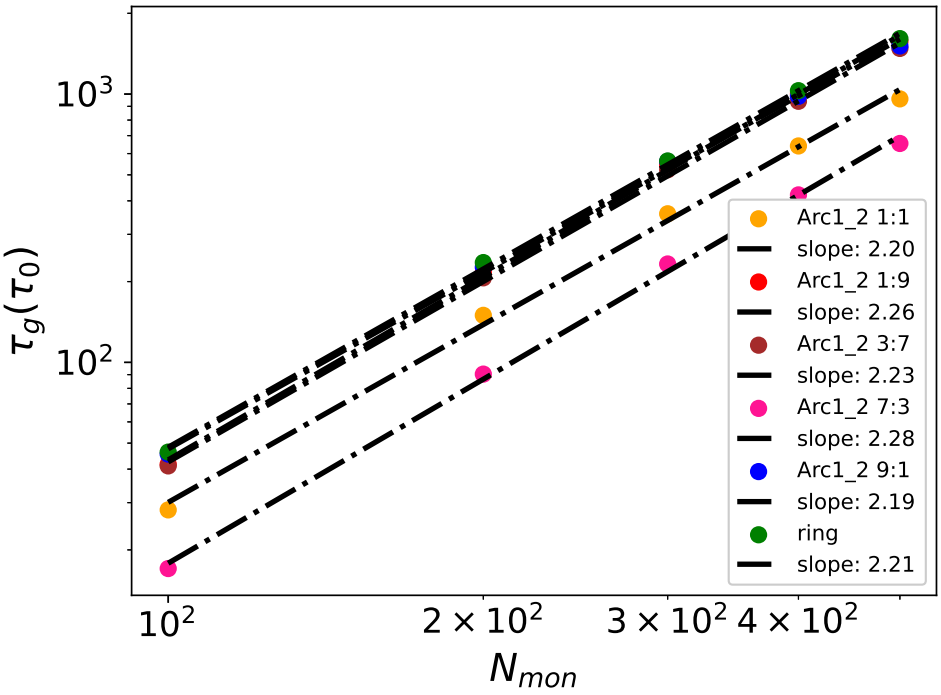

Figure 4.7: The graph shows scaling of C_g relaxation time for Symmetric Arc1_2, Arc1_2 of ratios 10%, 30%, 70%, and 90% against the total number of monomers. It follows $\tau_g \propto N^{2.2}$.

Here too the relaxation time increases with number of monomers as expected and shown in the figure 4.8.

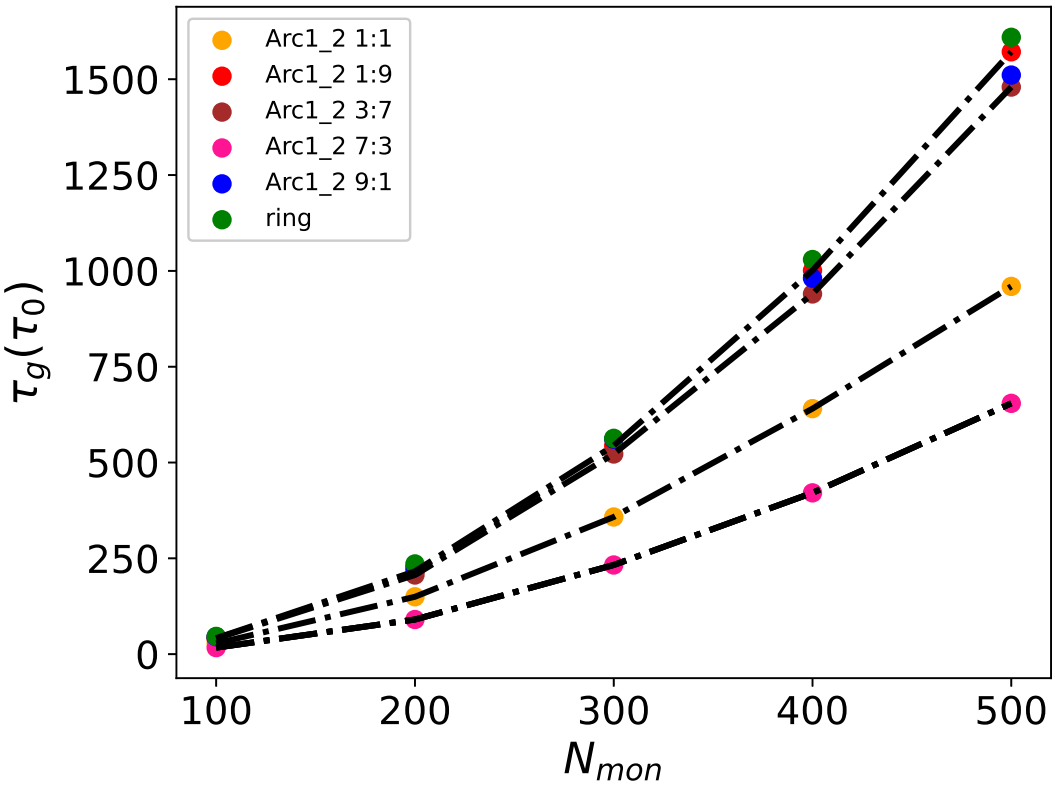

Figure 4.8: The graph shows C_g relaxation time for Symmetric Arc1_2, Arc1_2 of ratios 10%, 30%, 70%, and 90% with the total number of monomers. We see relaxation time increases as function of polymer length.

As similar to the case of Dumbbell architecture, here too we plot the relaxation time against the ratio graph in the figure 4.9. And as stated in the previous section, ratio of 0 indicates ring polymer of the given size. Here too we see a non-monotonous behavior of the relaxation time with the ratio of 7:3 or 70% shows the fastest relaxation time. For the case of ratio 7:3 all the three loops in Arc1_2 are of similar size. For example for the case of 100 total monomers, the two identical loops will have 35 monomers each and the third loop will have 30 monomers. Here we see that the Arc1_2 with ratio 9:1 has significantly larger relaxation time than that of Arc1_2 with ratio 7:3. And in ratio 9:1 the two identically sized loops are considerably larger than the third loop. For example, for the case of total number of monomers to be 100, the

two identical loops will have 45 monomers each and the third loop will have 10 monomers. One important thing to note here is that unlike the case of different dumbbell architectures, here all the Arc1_2 architectures despite the non-monotonous approach towards relaxation time of ring polymer, are faster than ring polymer.

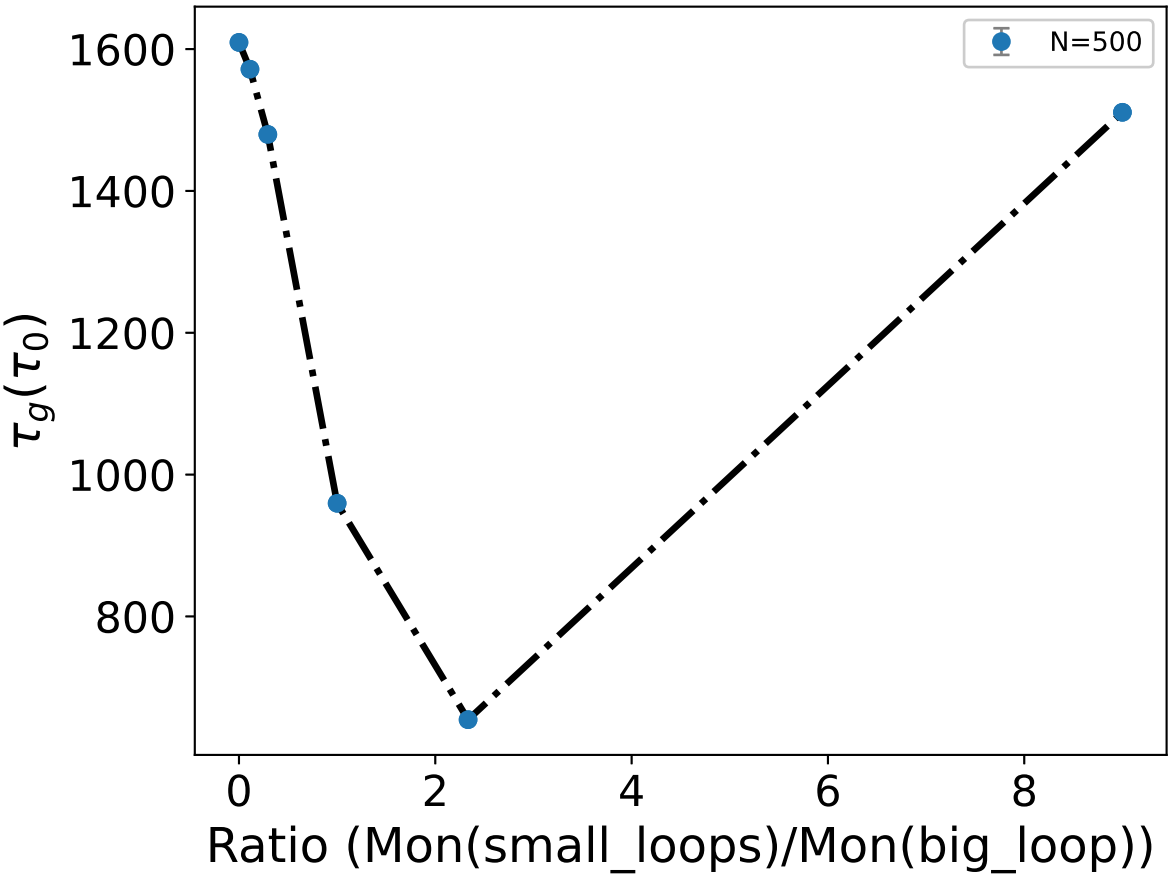

Figure 4.9: The graph shows C_g relaxation time for Symmetric Arc1_2, Arc1_2 of ratios 10%, 30%, 70%, and 90% with the total number of monomers equal to 500.

So the one conclusion about the relaxation time of different Arc1_2 architectures we draw from here is the following:

Ring Polymer > Arc1_2 1:9 > Arc1_2 9:1 > Arc1_2 3:7 > Symmetric Arc1_2 > Arc1_2 7:3

4.5 Other Polymer Architectures and Semiflexible polymer chain

We have also done similar study for relaxation time using the C_g method for all the different polymer architectures summarized in the table below.

Architecture (Monomers)	C_g **Relaxation Time**
SP_model (500)	194.073
Linear with side loops (190)	574.528
Linearly attached rings (200)	339.425
Flower_model (200)	109.757
Arc2_2 (500)	295.458

Table 4.1: C_g Relaxation times for various architectures with different monomer counts.

For the case of the semiflexible polymer chain, the relaxation time is summarized in the below table:

Monomers	**Bending Constant**	**Cg_relaxation**
200	50	10236.79
200	100	8111.70
200	200	8422.77

Table 4.2: C_g Relaxation of semiflexible polymer chains

Chapter 5

Relaxation of autocorrelation of Eigenvectors of Gyration Tensor (C_E)

5.1 Theory and Algorithm

5.1.1 Method description

The radius of gyration is a tensor quantity which contains information about the macroscopic size of the polymer in each direction. The radius of gyration tensor T_{ij} is given by:

$$T_{ij} = \frac{1}{N} \sum_{l=1}^{N} \left(x_{li} - \langle x_i \rangle\right) \left(x_{lj} - \langle x_j \rangle\right) \tag{5.1}$$

Here, N is the total number of monomers, and the indices i and j take values 1, 2, and 3 for each direction.

The sum of the eigenvalues of the radius of gyration tensor is the square of the scalar quantity radius of gyration, R_g, which we have used in the previous chapter. Now in this method to calculate the relaxation time we will perform time autocorrelation of the eigenvectors. We have performed the time autocorrelation for normalized eigenvectors associated with all

three - largest, lowest and the middle eigenvalue. Though the eigenvector associated with the largest eigenvalue gives very interesting results, which re-validates our results from the previous chapter and hence we investigate these properties further to arrive at a reasonable explanation for the dynamics that these architectures are showing.

The time autocorrelation function is given by :

$$C_E(dt) = \vec{e}(t + dt).\vec{e}(t) \tag{5.2}$$

where $e(\vec{t})$ are normalized eigenvector at a some arbitrary time t.

One important point to note here is that C_E is not particularly telling us about the rotational dynamics of the polymer. Because if it was it would be something like this:

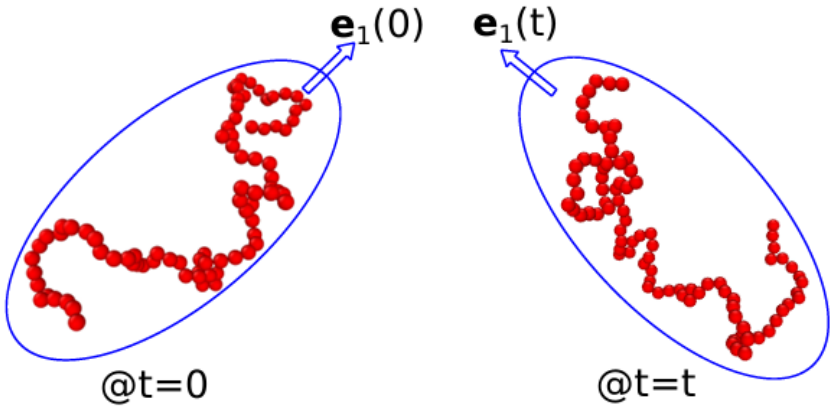

Figure 5.1: Rotational dynamics of a polymer.

But in order for this rotational dynamics to happen, the polymer will have to behave like a solid object where each point moves at the same angular velocity. This requires all the monomers of the polymer to move at the same angular velocity. This is not a realistic scenario in the case of a polymer. Thus C_E does not give rotational information about the system. Instead, C_E gives information about how quickly the polymer deforms in its shape.

5.1.2 Algorithm

Algorithm 5 Algorithm to calculate C_E

0: Initialize LAMMPS polymer simulation
0: Perform Monte Carlo simulation for 2000 steps
0: Perform Langevin Dynamics simulation for 2×10^8 iterations
0: **for** $t = 1$ to 2×10^8 **do**
0: Compute radius of gyration tensor
0: Diagonalize tensor to obtain eigenvalues and eigenvectors
0: Sort eigenvalues and eigenvectors
0: **end for**
0: **for** $t = 1$ to 2×10^8 **do**
0: **for** $dt = 1$ to 2×10^8 **do**
0: Compute $C_E = e(t+dt) \cdot e(t)$, where e is the eigenvector associated with the highest eigenvalue
0: Store C_E
0: **end for**
0: **end for**
0: **for** $i = 1$ to 20 **do**
0: Repeat the entire process
0: **end for**
0: Compute the average C_E over 20 runs for each corresponding timestep
=0

5.2 Linear Polymer, Ring Polymer, and Symmetric Dumbbell Polymer

Here $C_E(t)$ is also a decaying function with time. Because as the time interval between two eigen vectors increases , $\langle C_E(t)\rangle \to 0$. So, here also, similar to what we did in the last chapter, we fit the decaying function with an exponential function of the form $e^{-\frac{t}{\tau}}$, where τ is the relaxation time of the eigenvector. In the figure 5.2 below I have plotted $\langle C_E(t)\rangle$ to demonstrate the decaying function.

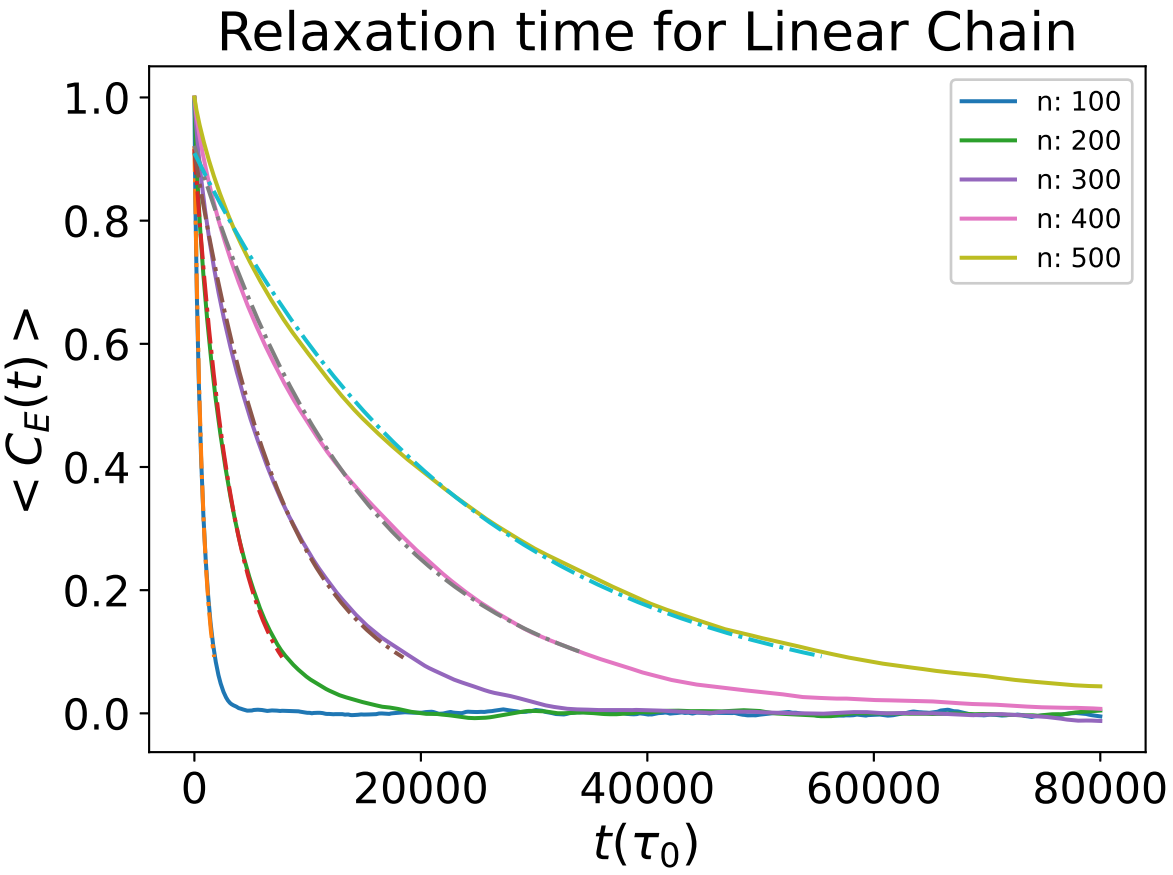

Figure 5.2: The graph shows decaying correlation function C_E as a function of time for different lengths of Linear Polymer Chain.

The figure represents the decaying $\langle C_E(t)\rangle$ curve for linear chain with length ranging from 100 to 500 monomers. The dotted line is the exponential function with which we fit the

data. Here too the relaxation time increases with increasing length of the polymer chain like in the previous methods. Now in order to extract the relaxation time from the exponential function we need to take the linear range of the data. This is because we are fitting the graph with $C_E(t) = e^{-\frac{t}{\tau}}$. So plotting the semi-log graph with $\log C_E(t)$ on the y-axis and time on the x-axis, we should get a linear line whose inverse of slope can give us the relaxation time. So when we plot this semi-log plot, we look for this linear line regime and extract the slope of the linear line to find out the relaxation time. This has been explicitly shown in the figure 5.3 below for the case of linear chain with 100 and 200 monomers.

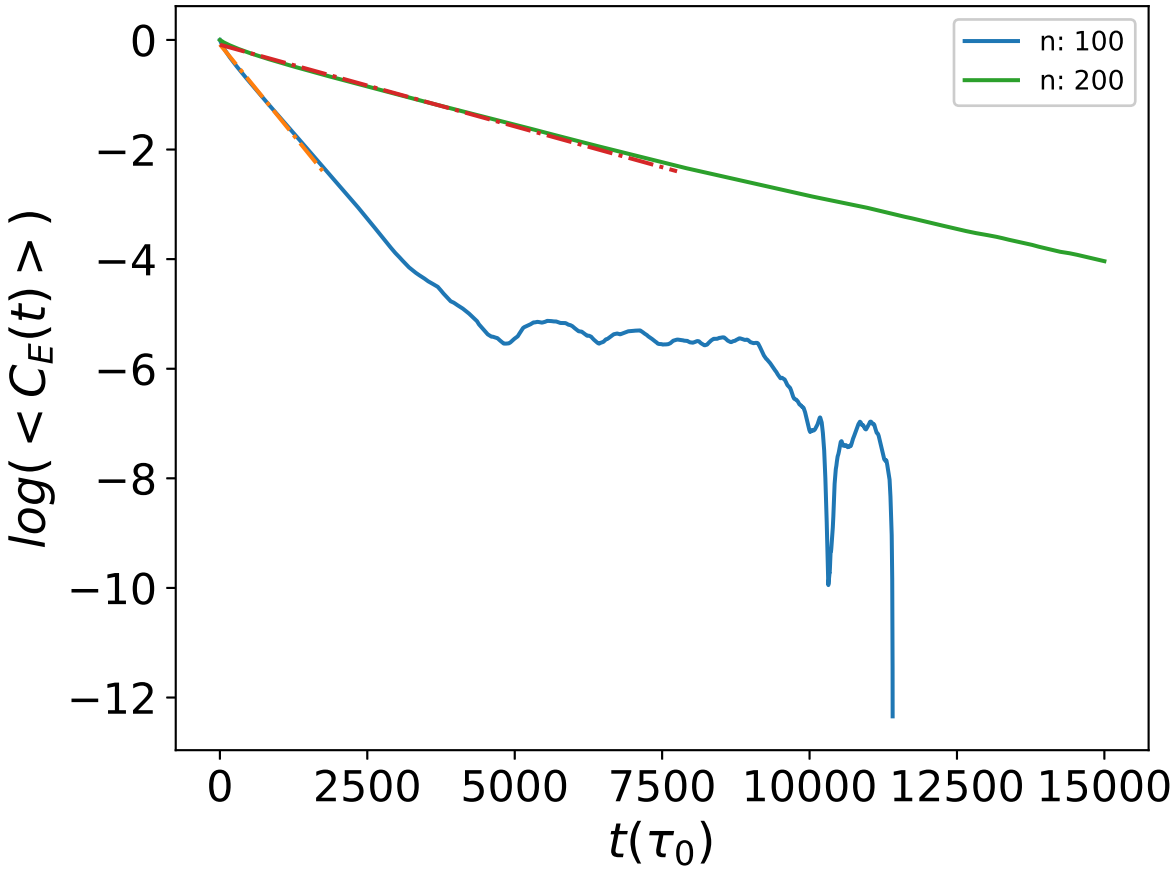

Figure 5.3: The graph shows sem-log plot for $\langle C_E(t) \rangle$ for linear chain with N=100 and 200. It is fitted with the linear regime we use to extract relaxation time.

Now that we know that relaxation time of these eigenvectors increase with increase with the chain length of the polymer, we plot the graph of relaxation time against number of

monomers on the log scale to get the definitive scaling relation. In the figure 5.4 below, we do that for linear polymer chain for length 100 to 1000 monomers.

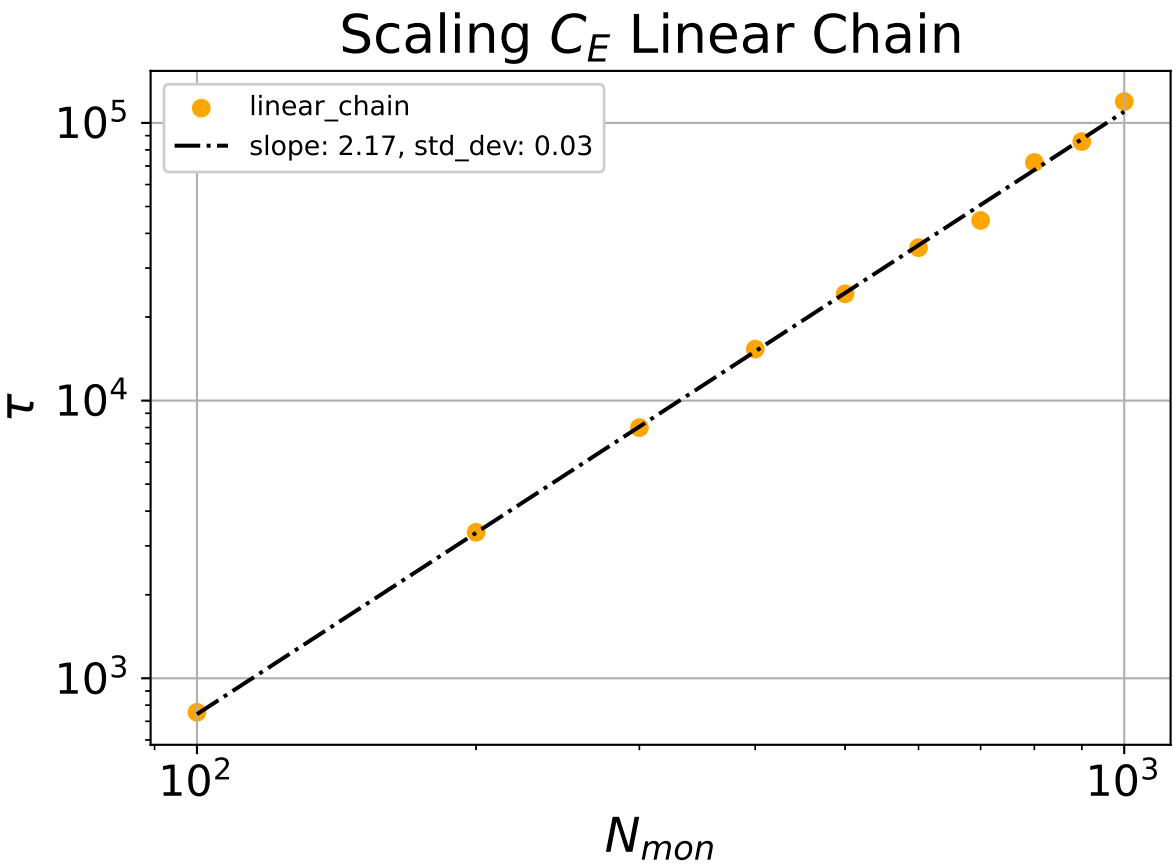

Figure 5.4: The graph shows scaling between relaxation time and the number of monomers

Here we see a scaling of :

$$\tau \propto N^{2.17} \tag{5.3}$$

This is similar to the scaling of $\tau \propto N^{2.2}$ that we got for the end-to-end vector and C_g relaxation method. This also reaffirms the validity of this method that we will use to calculate relaxation time for more complex topologies of the polymers. This also establishes another method that does not depend on the structural details of the polymer. We will now use C_E relaxation method to study the dynamics of modified topologies.

In the figure 5.5 below, we plot the scaling relation of linear chain, ring polymer, symmetric dumbbell, and symmetric Arc1_2 architecture of polymer length ranging from 100 to 500 monomers.

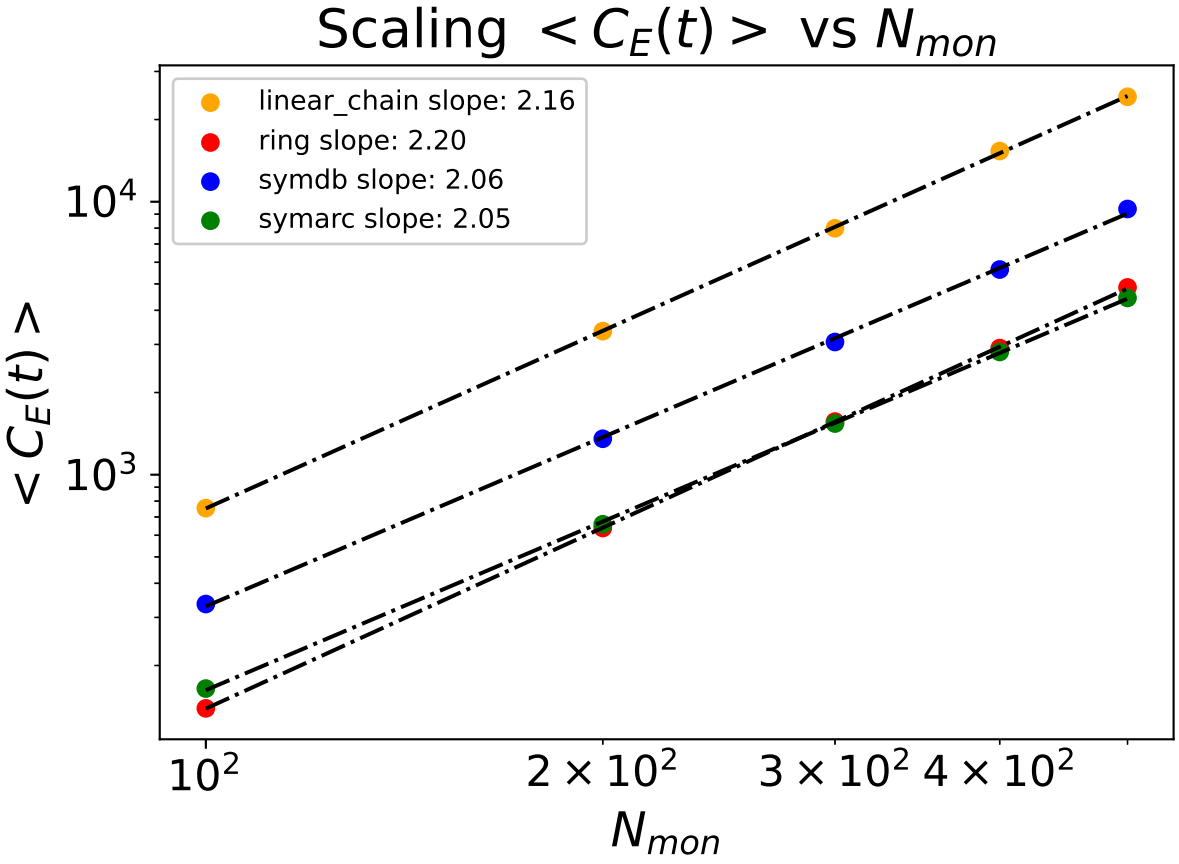

Figure 5.5: The graph shows scaling between C_E relaxation time and the number of monomers for linear chain, ring polymer, symmetric Dumbbell, and symmetric Arc1_2 polymer.

In the above figure, we again see that ring polymer, symmetric dumbbell, and symmetric Arc1_2 follow similar scaling relation between relaxation time and number of monomers. And here too, we have not used too high values of polymer length because it is computationally very expensive, both in terms of storage and time. Furthermore, we observe that the linear chain has the highest relaxation time and the relaxation time of dumbbell lies between that of ring polymer and linear chain for a given polymer length. This is the same trend that we obtained from end-to-end vector relaxation method and C_g relaxation method. We also

notice that symmetric Arc1_2 and ring polymer have approximately same relaxation time.

The trend in C_E relaxation time that we obtain can be summarized as follows:

Linear Polymer > Symmetric Dumbbell > Ring Polymer ≈ Symmetric Arc1_2

5.3 Asymmetric Dumbbell Polymers

Similarly to the previous chapter, we systematically study the C_E relaxation time for the same asymmetric dumbbell architectures. We investigate the relation between these unequal loop sizes to the relaxation time of eigenvectors of the polymer.

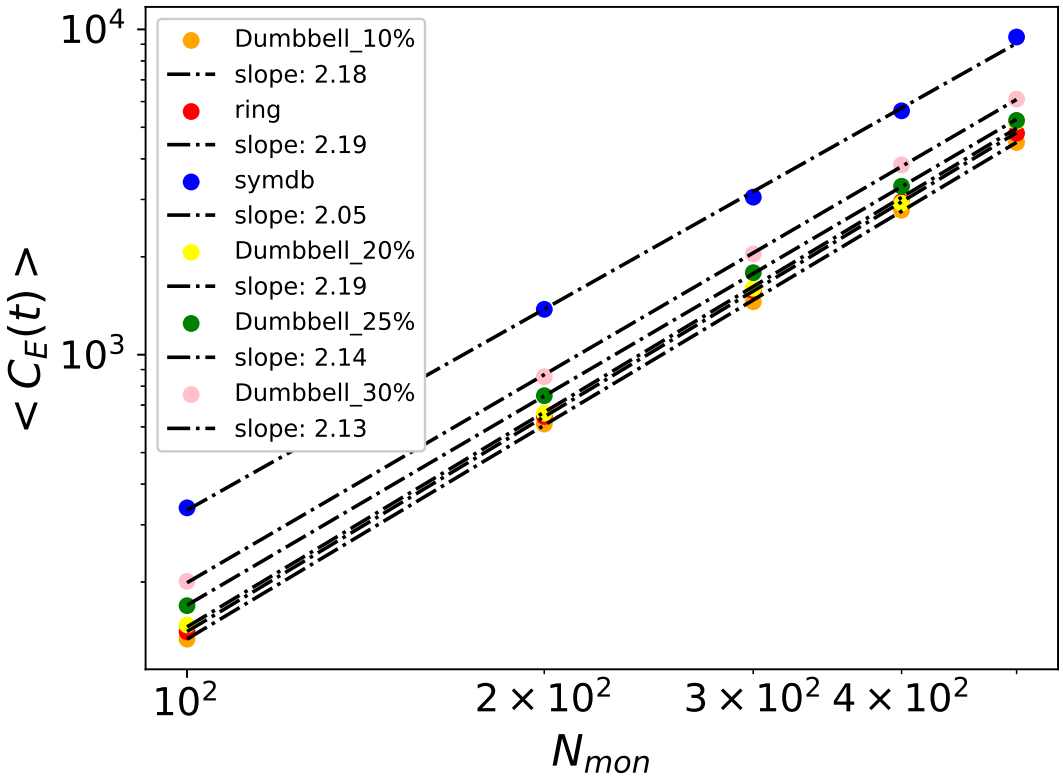

Figure 5.6: The graph shows scaling of C_E relaxation time for Symmetric Dumbbell, Dumbbell of ratios 10%, 20%, 25%, and 30% with the total number of monomers.

In the figure 5.6 , we plot the scaling relation of C_E relaxation time against monomers for different ratios of dumbbell architectures. The y-axis is the C_E Relaxation time and x-axis is the number of monomers with the graph is drawn in logarithmic scale and this gives the scaling relation similar to what we obtained in the previous section.

In figure 5.7 we show that the relaxation time increases with the number of monomers and the difference is signified for polymers with higher number of monomers. Here we see that the symmetric dumbbell polymer takes the highest time to relax as compared to other ratios of dumbbell architecture. We also note that dumbbell with ration 10% takes the least amount of time to relax and is faster than ring polymer for all the polymer lengths.

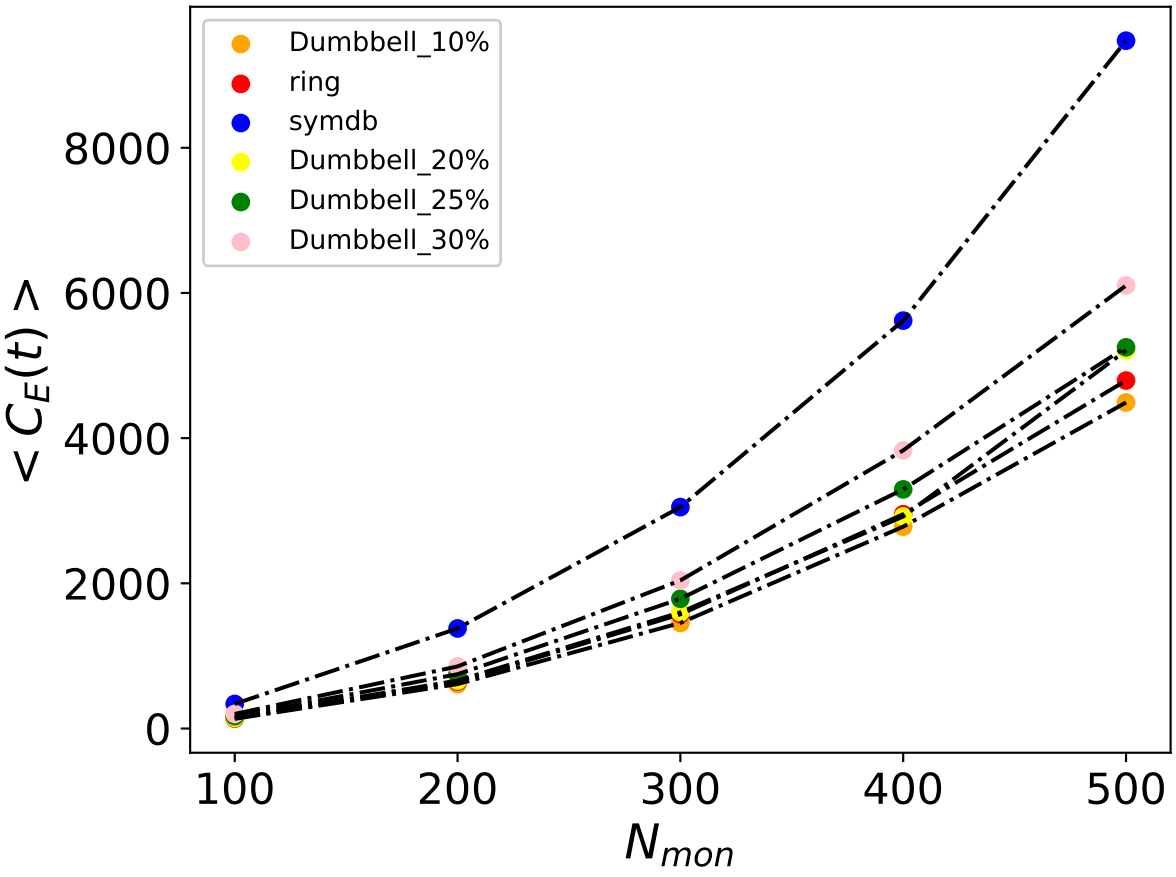

Figure 5.7: The graph shows C_E relaxation time for Symmetric Dumbbell, Dumbbell of ratios 10%, 20%, 25%, and 30% with the total number of monomers. Relaxation time increases with polymer length.

In the figure 5.8 below represents a plot of relaxation time against ratios graph for different dumbbell architectures for the case of total 500 monomers. The ratio basically is Monomers in small loop divided by monomers in the big loop. So ratio 0 indicates no small loop or essentially just a ring polymer. Similarly, ratio of 1 indicates a symmetric Dumbbell polymer.

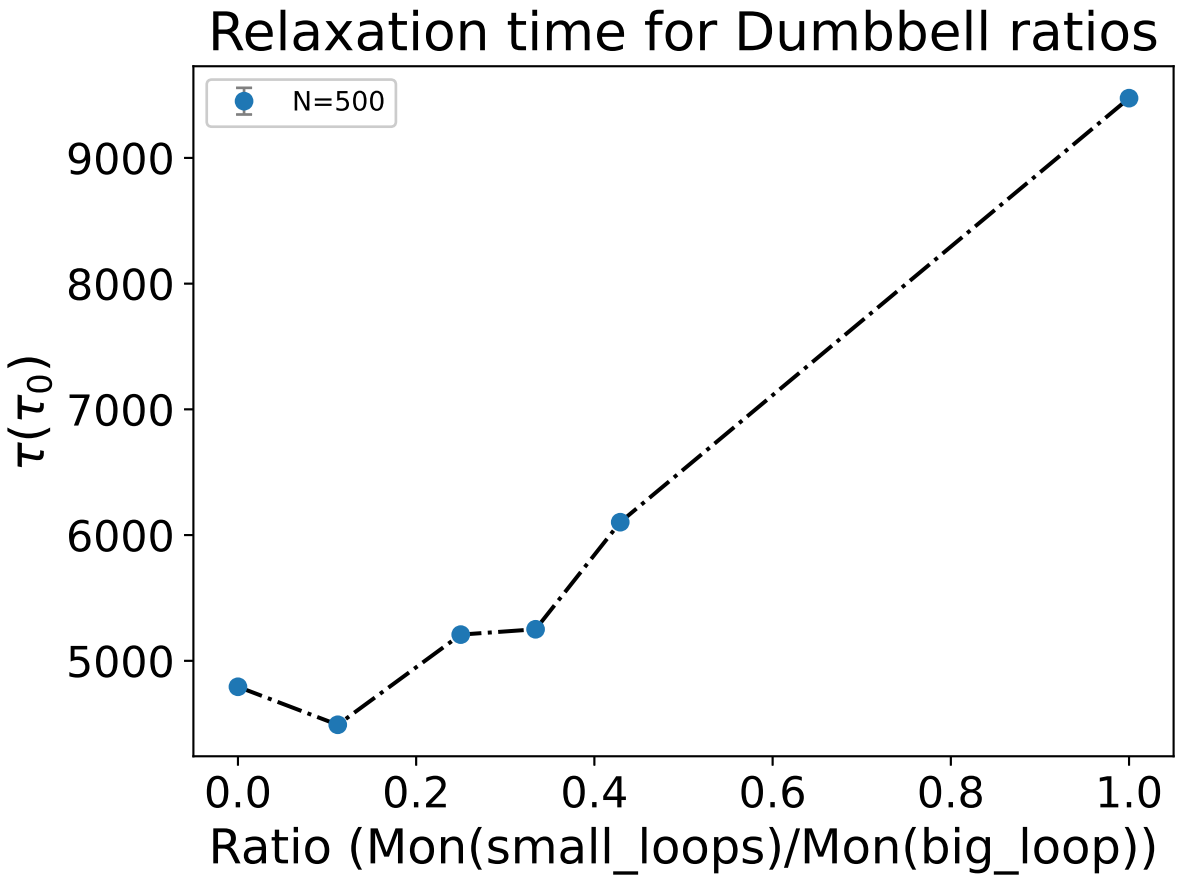

Figure 5.8: The graph shows C_E relaxation time for Symmetric Dumbbell, Dumbbell of ratios 10%, 20%, 25%, and 30% with the total number of monomers equal to 500.

Here we again see that non-monotonous approach towards the relaxation time of ring because as I said before dumbbell with ratio 10% takes less amount of time than that of ring polymer. This is also equivalent to the observation we made with C_g relaxation method where both 10% and 20% showed lesser relaxation time than ring. The reproducibility of this result affirms the fact that this non-monotonous behavior in relaxation time does not arise from the bias towards use of certain method to calculate it, instead it is general result which

requires an explanation. The trend in C_E relaxation time for different dumbell ratios can be summarized as follows:

Symmetric Dumbbell > Dumbbell 3:7 > Dumbbell 1:3 > Dumbbell 1:4 > Ring Polymer > Dumbbell 1:9

5.4 Asymmetric Arc1_2 Polymers

Now we will use C_E relaxation method to carry out similar investigation for different ratios of Arc1_2 polymers. The definition of ratios stays the same that we defined in the last chapter.

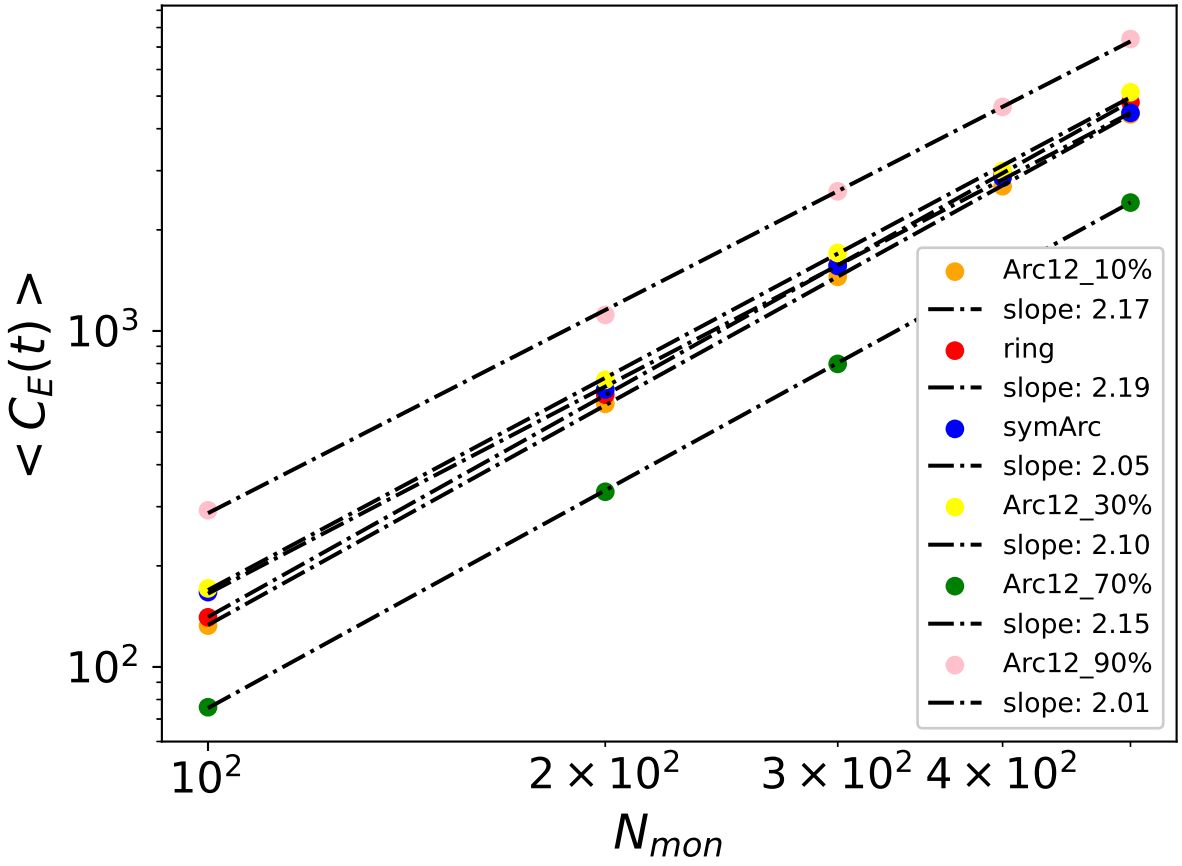

Figure 5.9: The graph shows scaling of C_E relaxation time for Symmetric Arc1_2, Arc1_2 of ratios 10%, 30%, 70%, and 90% against the total number of monomers.

In figure 5.9 we plot the scaling relations of C_E relaxation time with number of monomers for different ratios. Here we again see similar scaling relation between relaxation time and number of monomers that we saw for different architectures using the C_E method. And it is also similar to the scaling relation that we obtained when we calculated relaxation time using different methods.

In figure 5.10 we plot the C_E relaxation time with number of monomers. It showcases the property that for Arc1_2 polymer as well, the relaxation time increases with number of monomers. We can see that Arc1_2 with ratio 10% takes the highest time to relax. And Arc1_2 with ratio 70% takes the lowest time to relax. This is the same thing that we observed using C_g relaxation method as well.

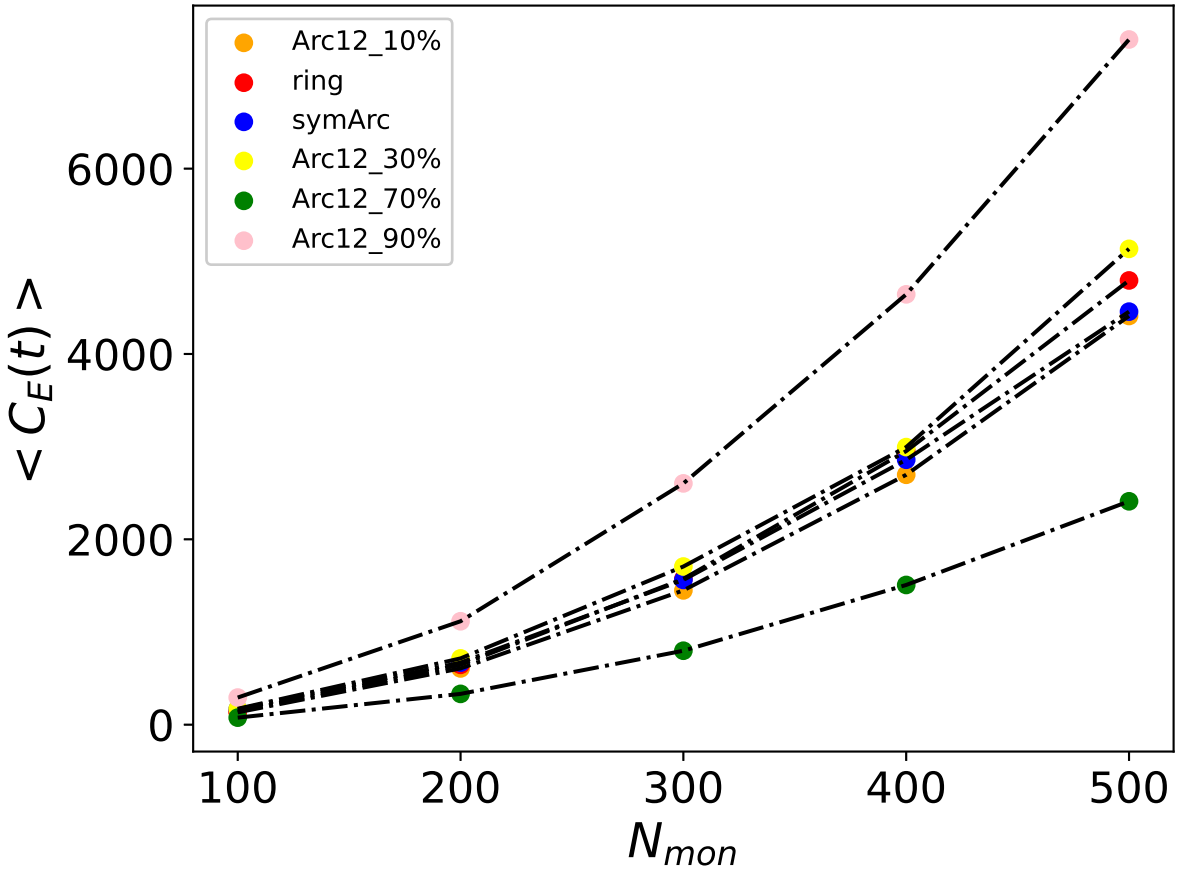

Figure 5.10: The graph shows C_E relaxation time for Symmetric Arc1_2, Arc1_2 of ratios 10%, 30%, 70%, and 90% against the total number of monomers.

In the figure 5.11 below we plot C_E relaxation time for different ratios of Arc1_2 polymer with total number of monomers equal to 500. Again like C_g method we see non-monotonous approach to ring polymer case here as well. Arc1_2 with ratio 70% has significantly less relaxation time compared to other ratios.

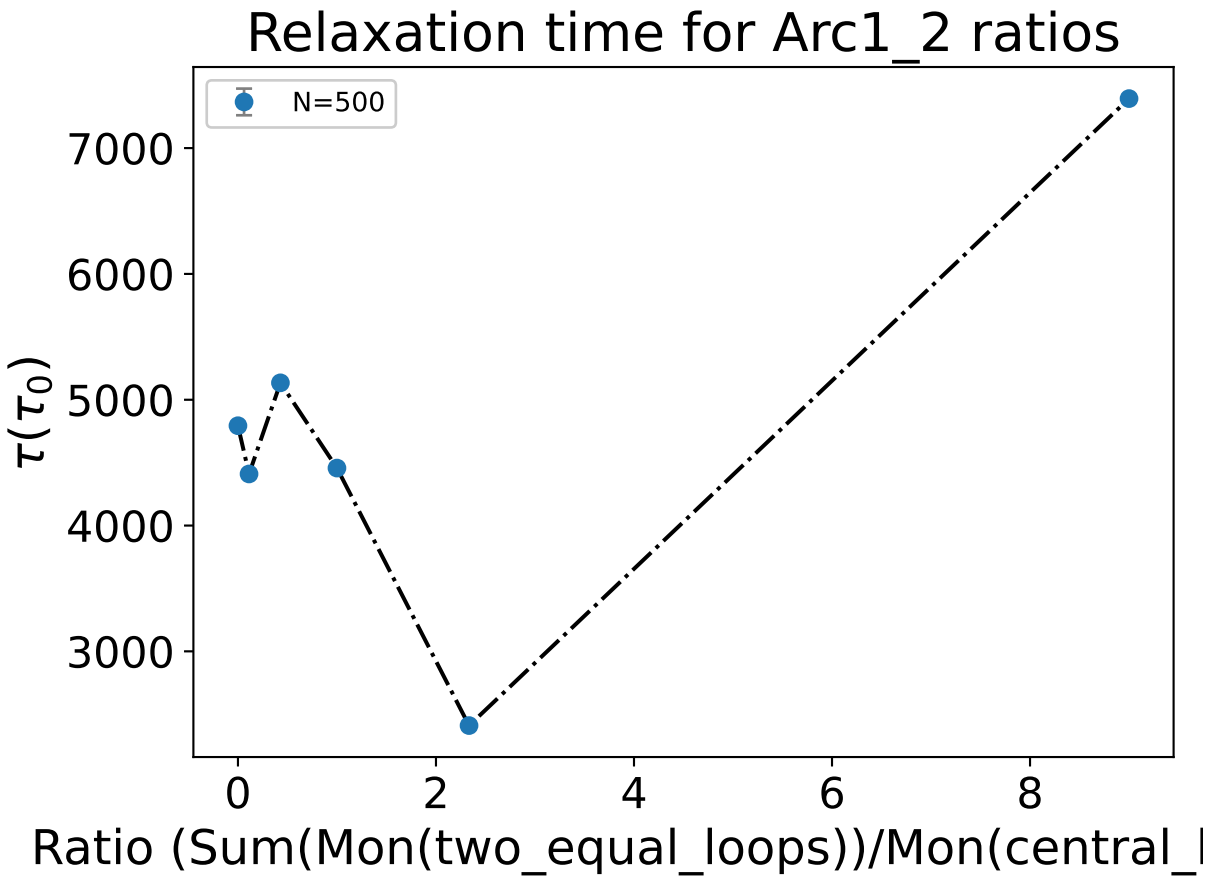

Figure 5.11: The graph shows C_E relaxation time for Symmetric Arc1_2, Arc1_2 of ratios 10%, 30%, 70%, and 90% with the total number of monomers equal to 500.

So to summarize, the C_E relaxation time trends for different Arc1_2 ratios are as follows:

Arc1_2 9:1 > Arc1_2 7:3 > Symmetric Arc1_2 > Arc1_2 3:7 > Ring Polymer > Arc1_2 1:9

5.5 Other Polymer Architectures and Semiflexible polymer chain

We have also done similar study for relaxation time using the C_E method for all the different polymer architectures summarized in the table below.

Architectures (Monomers)	**Eigenvector Relaxation Time**
SP_model (500)	756
Linear with side loops (190)	2013
Linearly attached rings (200)	1537
Flower_model (200)	359
Arc2_2 (500)	892

Table 5.1: Eigenvector relaxation times for various architectures

For the case of semiflexible chain with different bending energy constants, C_E relaxation time is summarized below.

Monomers	**Bending Constant**	**Highest_eigen**
200	50	290021.84
200	100	277984.40
200	200	259696.32

Table 5.2: Relaxation of semiflexible polymer chains

Chapter 6

Anisotropy and its relation to relaxation dynamics

6.1 Definition and Algorithm

Mathematically, Anisotropy is defined by following formula:

$$A_d = \frac{\sum_{i>j}^{d} \left\langle \left(R_i^2 - R_j^2\right)^2 \right\rangle}{(d-1)\left\langle \left(\sum_{i=1}^{d} R_i^2\right)^2 \right\rangle} \tag{6.1}$$

Here d is the dimension of the system in which we are working, for our case $d = 3$. R_i^2 are the eigenvalues of the radius of gyration tensor defined as follows:

$$T_{ij} = \frac{1}{N}\sum_{l=1}^{N} \left(x_{li} - \langle x_i \rangle\right)\left(x_{lj} - \langle x_j \rangle\right) \tag{6.2}$$

Here, N is the total number of monomers, and the indices i and j take values 1, 2, and 3 for

each direction.

Intuitively, the shape is the most obvious physical property to observe for a physical object like a polymer. The macroscopic shape is often dictated by the microscopic principles that controls its dynamics and formation. The shape of a polymer is also interesting to investigate because shape of a polymer is result of a random process and studying it would also help in understanding the nature of the underlying random process. It would also give us information about the effect of additional constraints we put on degree of freedom by introducing crosslinks on overall shape of the polymer. Anisotropy defined above is a quantitative measure of the shape of a physical object. It takes values between 0 and 1, where 0 being perfectly spherical and 1 being perfectly anisotropic rod-like structure.

6.1.1 Algorithm

Algorithm 6 Monte Carlo and Langevin Dynamics Simulation for Anisotropy Calculation

1: **Initialize** polymer configuration.
2: Run Monte Carlo simulation for 2000 timesteps.
3: Run Langevin Dynamics simulation for 1.5×10^6 timesteps (Equilibration Phase, no data collection).
4: Run Langevin Dynamics simulation for 2×10^8 timesteps:
5: **for** each timestep **do**
6: Compute the gyration tensor.
7: Diagonalize the gyration tensor to obtain eigenvalues $(R_1)^2, (R_2)^2, (R_3)^2$.
8: Compute anisotropy using the given formula: $A_d = \frac{\sum_{i>j}^{d} \left\langle \left(R_i^2 - R_j^2\right)^2 \right\rangle}{(d-1)\left\langle \left(\sum_{i=1}^{d} R_i^2\right)^2 \right\rangle}$
9: **end for**
10: Compute the average anisotropy over all timesteps.
11: Repeat the entire process 20 times.
12: Compute the final anisotropy as the average of 20 independent runs. =0

In order to diagonalize the gyration tensor and calculate its eigenvalues and eigenvectors, we use an inbuilt package in Fortran. The results we get using this inbuilt package is also verified by manually checking it for certain cases. Inbuilt package is preferred because it is computationally faster when used over very long runs that we do here.

6.2 Fractal property of Anisotropy

Now before we move further, one important thing to realize is that a polymer in a freely rotating chain model is essentially a random walk. Let's say a random walker starts from origin and keeps a bead at the origin, then it hops to the next position and keeps another bead at that position. Now he also connects the bead it places at that particular time step to the bead he placed at the previous time step If he then does a random walk for N steps in total, one gets a linear freely rotating polymer chain with N monomers in total. If there is a constraint due to excluded volume interaction that the monomers cannot come very close to each other then we move into the regime of self-avoiding random walk, where the random walker cannot return to the position it previously held.

Now when we talk about anisotropy of the shape of a polymer, we are essentially talking about anisotropy in the shape of envelope enclosing the trajectory of a random walker. The shape of such an object can be obtained from ensemble average of of the eigenvalues of the gyration tensor. The eigenvalues can be found at every time step and then ordered according to the magnitude and then can be averaged over. By doing this the one can persist the average intrinsic anisotropy of an object and it will not vanish due to orientational averaging. This has been done both analytically and numerically in the case of 3-dimensions, both for unrestricted random walks and restricted self-avoiding random walks. In the case of long unrestricted random walks walks, one achieves a limiting ratio of eigenvalues as follows:

$$\langle R_1^2 \rangle : \langle R_2^2 \rangle : \langle R_3^2 \rangle = 11.80 : 2.69 : 1.00 \tag{6.3}$$

This suggests that contrary to what one might imagine and expect, the shape of a simple random walk is not spherical. These eigenvalues can be thought of as the length of major and minor axes, and since all the eigenvalues are not identical, the length of axes is not same in each direction and hence it is not spherical in shape. One more interesting point to note here is that this ratio does not depend on the number of steps a random walker takes, thus, this same ratio and anisotropy prevails for all total number of steps. This is what we call a fractal property of a random walk. This anisotropy holds true in all directions, obviously with different sets of ratio in each dimension, but still not spherical as per expectation. In

our simulations as well, we first verify our code by reproducing this anisotropy ratio for unrestricted simple random walk and we do this by finding this ratio for a simple linear chain without excluded volume interaction. We do this for lengths ranging from 100 to 1000 monomers which is equivalent to 100 to 1000 total steps of a random walk. We get to see the same ratio as above and the average taken over the ratio we obtained for each of these lengths is summarized in the table below.

Topology	$\langle(R_1)^2\rangle$	$\langle(R_2)^2\rangle$	$\langle(R_3)^2\rangle$
Linear Polymer noEV	11.69	2.69	1.00
Linear Polymer with EV	14.53	2.97	1.00
Ring Polymer	7.19	2.88	1.00
Symmetric Dumbbell	6.86	2.17	1.00
Dumbbell 10%	7.06	2.86	1.00
Dumbbell 20%	6.96	2.72	1.00
Dumbbell 25%	6.85	2.62	1.00
Dumbbell 30%	6.85	2.51	1.00
Symmetric Arc1_2	5.38	2.16	1.00
Arc1_2 1:9	7.17	2.90	1.00
Arc1_2 3:7	6.65	2.54	1.00
Arc1_2 7:3	4.87	2.31	1.00
Arc1_2 9:1	6.27	2.12	1.00
Linearly attached rings	7.66	2.14	1.00
Linear chain with side loops	13.4	2.82	1.00
Flower Model	6.43	2.92	1.00
Arc2_2	3.36	1.97	1.00
SP model	3.24	1.92	1.00

Table 6.1: Eigenvalue Ratios for Different Topologies

In the figure 6.1 below we show anisotropy against number of monomers. The straight line depicts the fractal nature where anisotropy is independent of length of the polymer.

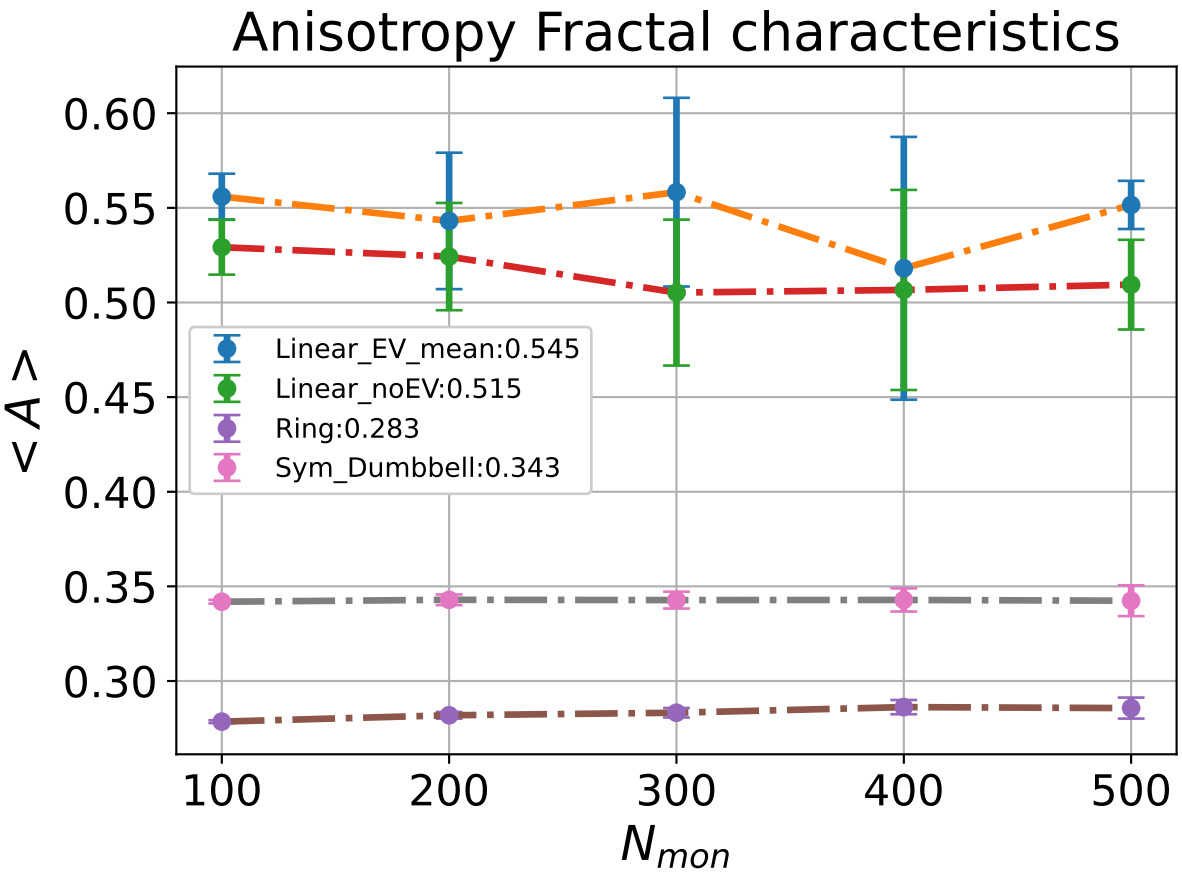

Figure 6.1: Fractal nature of anisotropy - linear chain with and without EV, ring polymer and Symmetric Dumbbell polymer.

In the figure we only show this property for linear chain with and without excluded volume interaction, ring polymer, and Symmetric dumbbell, but this property in general holds true for all the different polymer topologies that we work with as well.

For the case of random walks without excluded volume interaction, theoretical calculations for exact value of anisotropy gives following formula. For linear chain:

$$A_d = \frac{2(d+2)}{5d+4} \tag{6.4}$$

For ring polymer:

$$A_d = \frac{d+2}{5d+2} \tag{6.5}$$

For the case of polymers with excluded volume interaction, renormalization group calculations by Aronovitz and Nelson gives following results for 4-ϵ dimensions for linear chains:

$$A_d = \frac{2(d+2)}{5d+4} + 0.008\epsilon \tag{6.6}$$

Here $\epsilon = 1$ for the case of 3 dimensions and d denotes the dimension in above formulae. The values predicted by these formulas are very close to the values that we have plotted in the figure 6.1.

6.2.1 Algorithm

Algorithm 7 Monte Carlo and Langevin Dynamics Simulation for Anisotropy Ratio Calculation

1: **Initialize** polymer configuration.
2: Run Monte Carlo simulation for 2000 timesteps.
3: Run Langevin Dynamics simulation for 1.5×10^6 timesteps (Equilibration Phase, no data collection).
4: Run Langevin Dynamics simulation for 2×10^8 timesteps:
5: **for** each timestep **do**
6: Compute the gyration tensor.
7: Diagonalize the gyration tensor to obtain eigenvalues $(R_1)^2, (R_2)^2, (R_3)^2$.
8: Sort eigenvalues such that $(R_1)^2 \leq (R_2)^2 \leq (R_3)^2$.
9: Compute the anisotropy ratio: $(R_1)^2 : (R_2)^2 : (R_3)^2$.
10: **end for**
11: Compute the average anisotropy ratio over all timesteps.
12: Repeat the entire process 20 times.
13: Compute the final anisotropy ratio as the average of 20 independent runs. =0

6.3 Dumbbell Polymers

For the case of Dumbbell Polymers, we saw that for a given length of polymer, the relaxation time vs ratio graph shows non-monotonous approach towards relaxation time to that of ring. This was conveyed through figure 4.6 and figure 5.8. Now in the figure 6.2 I plot the anisotropy of different dumbbell polymer ratios against the ratio to compare it with the relaxation time vs ratio plot. Now this was done here keeping the total length of all the different ratios of dumbbell polymer fixed to be 400 monomers. We observe that in this graph as well we see this non-monotonicity similar to what we saw in the relaxation time vs ratio graph in both the methods. This suggests that anisotropy and relaxation dynamics are correlated.

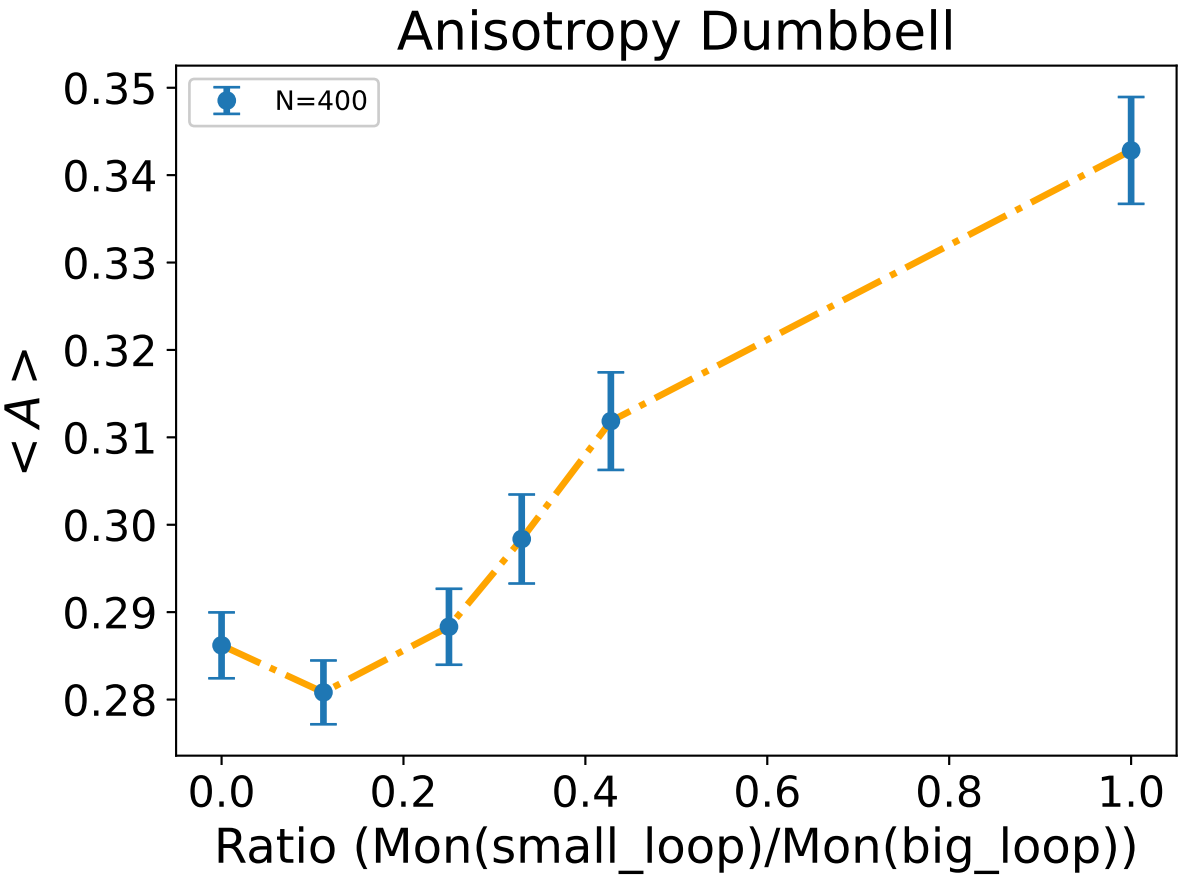

Figure 6.2: Average anisotropy vs different ratios of dumbbell polymers.

6.4 Arc1_2 Polymers

We do the same kind of analysis that we did for the Dumbbell polymers with all the different ratios of Arc1_2 polymers. In the figure 6.3 below we see the average anisotropy vs ratio graph for Arc1_2 polymers. Here to we observe the same type of behavior that we saw in relaxation time vs ratio graph in figure 5.11. This again suggests that the anisotropy and relaxation time are somehow correlated. It might be the case that anisotropy dictates or drives the dynamics of these architectures but the causation is not directly implied. Here we just put forward the correlation between relaxation time and the anisotropy of a polymer architecture.

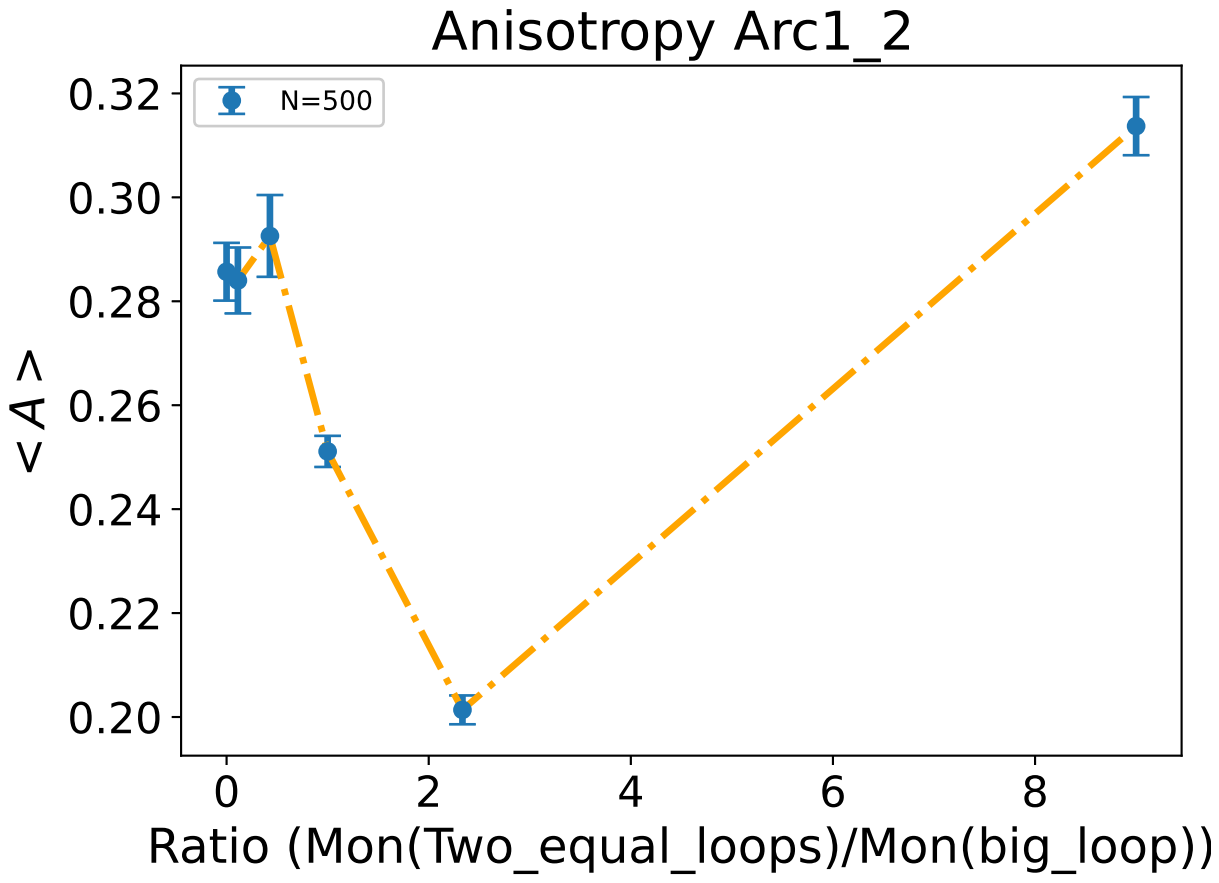

Figure 6.3: Average anisotropy vs different ratios of Arc1_2 polymers.

6.5 Scaling Relations

Scaling relations are one of the most central concepts in statistical mechanics. From the previous section we know that anisotropy and relaxation dynamics of the polymers are correlated. Hence, here we will draw the scaling between them. First we will do this using the relaxation time we obtained using the C_g method, which denoted the correlation in fluctuations of radius of gyration. Later, we will do draw the correlation between anisotropy and relaxation time using C_E method, which denoted the time autocorrelation of the eigenvectors of the gyration tensor. Note that in both the cases the anisotropy values are the same.

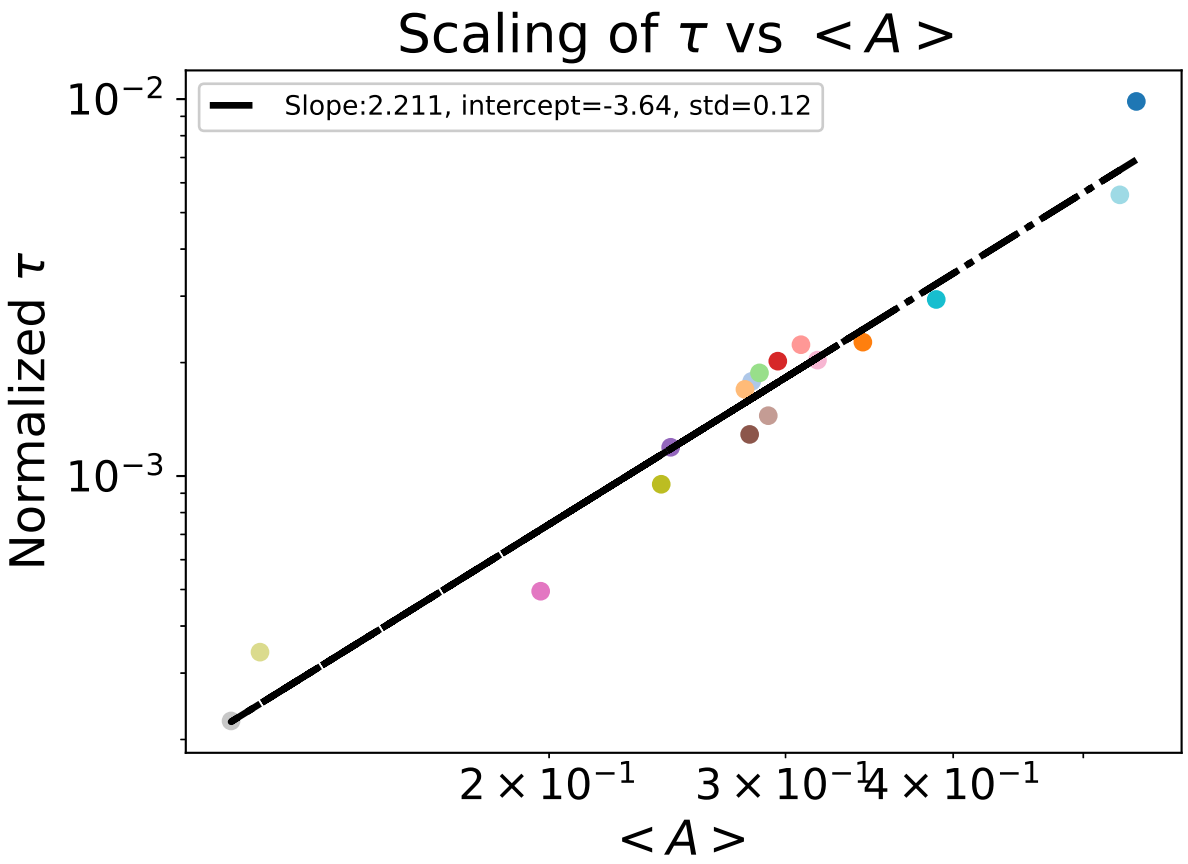

Figure 6.4: Scaling between normalized C_g relaxation time and average anisotropy.

In the figure 6.4 we have used Normalized relaxation time. This normalization has been done by dividing the relaxation time by $N^{2.2}$, where N is the length of that polymer. For

example for the case of linear polymer of length 100 to 500, we divide relaxation time by corresponding length and then take average of the 5 normalized time we obtained and use that as the normalized C_g relaxation time of the linear chain. This has been done for all the type of architectures. Hence, each data point on the graph represents different type of architecture.

We see the scaling relation of:

$$\tau_g \propto N^{2.2} \langle A \rangle^{2.2} \tag{6.7}$$

In figure 6.5 we plot the similar thing using the C_E relaxation time.

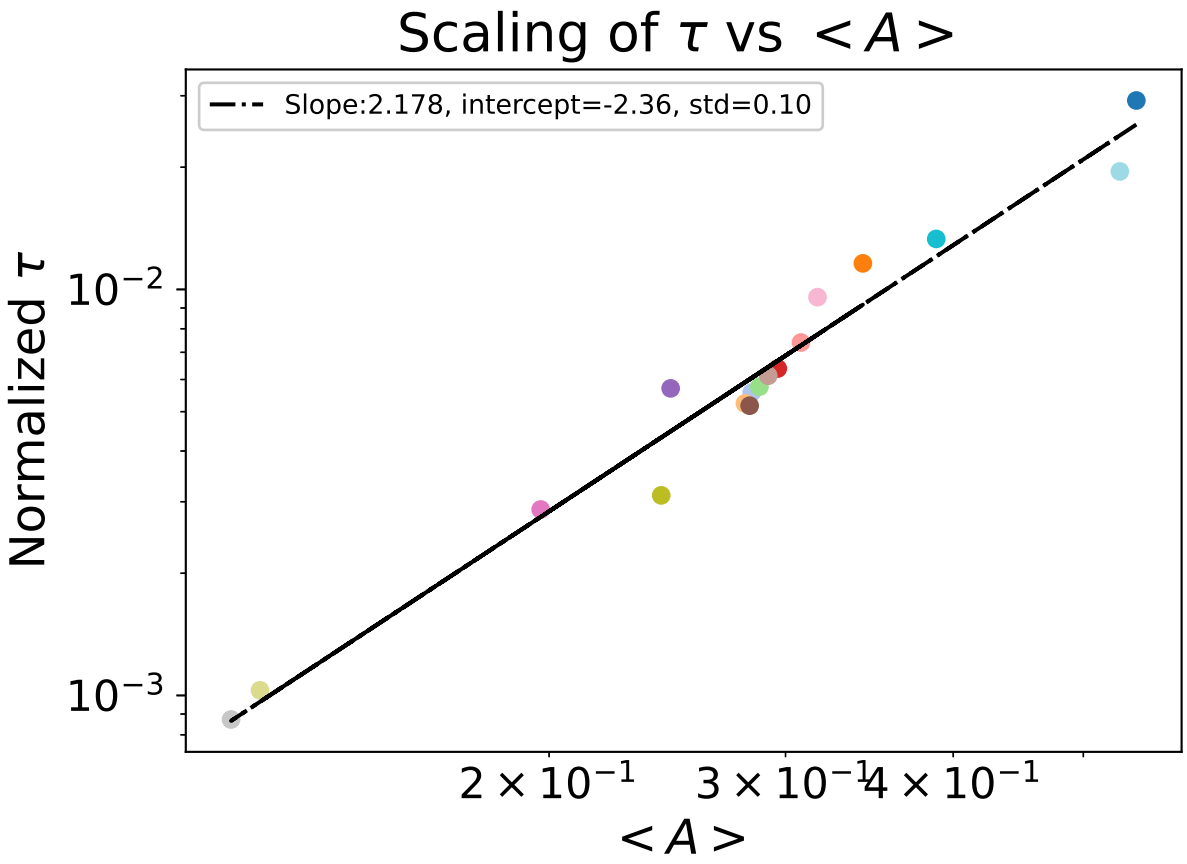

Figure 6.5: Scaling between normalized C_E relaxation time and average anisotropy.

Here too the scaling between relaxation time, length of the polymer and average anisotropy is give as:

$$\tau \propto N^{2.2} \langle A \rangle^{2.2} \tag{6.8}$$

In conclusion, here we establish a new scaling relation between the relaxation time, length of polymer and the average anisotropy in the fundamental theory of polymer physics. This is not only important in the true fundamental sense which relates the shape of the polymer to its relaxation dynamics but also holds practical advantage in calculating relaxation time. Now in order to estimate relaxation time of any topologically modified polymer, we can directly calculate the anisotropy and get a reasonable estimate which is computationally very fast compared to calculating correlations which are computationally very expensive both in storage and the amount of time required.

We observe that the polymer with the lowest relaxation time also has the lowest anisotropy. One possible explanation for this might be that since we are performing Langevin dynamics simulations, we have fixed the temperature and hence the velocity profile or range of the monomers. But the contraints that we add on the topology by introducing the crosslinks changes the range in position space the polymer can take. Hence with lower range of positions, the phase space volume decreases and hence it takes less time for the polymer to explore the phase space and approach equilibrium.

Chapter 7

Supplementary Information

7.1 C_g relaxation time data

The end-to-end vector relaxation time data for linear chain in comparison with C_g method are in the following table.

Monomers	**End-to-End Vectors Relaxation Time**			**C_g Relaxation Time**		
	Linear Chain	**Ring Polymer**	**Dumbbell 1:1**	**Linear Chain**	**Ring Polymer**	**Dumbbell 1:1**
100	1092	461	579	247	46	55
200	5130	1995	2565	1228	236	280
300	12162	4740	6366	2982	568	697
400	23754	8810	12078	5500	1041	1238
500	38147	14279	20415	8525	1630	1853

Table 7.1: End to End vector relaxation time and Cg relaxation time comparison.

The C_g relaxation time data for ring polymer and different ratios of dumbbell polymers:

Monomers	Ring Polymer	Dumbbell 1:1	Dumbbell 1:9	Dumbbell 1:4	Dumbbell 1:3	Dumbbell 3:7
100	46	55	42	44	48	52
200	236	280	218	238	250	263
300	568	697	522	572	616	655
400	1041	1238	931	999	1068	1139
500	1630	1853	1482	1531	1664	1752

Table 7.2: C_g relaxation times for different dumbbell ratios and ring.

The C_g relaxation time data for ring polymer and different ratios of Arc1_2 polymers:

Monomers	Ring Polymer	Arc1_2 1:9	Arc1_2 3:7	Arc1_2 1:1	Arc1_2 7:3	Arc1_2 9:1
100	46	42	41	28	17	46
200	236	216	207	150	90	226
300	568	544	522	358	233	561
400	1041	1001	940	641	421	981
500	1630	1572	1480	960	654	1511

Table 7.3: C_g relaxation times for different ratios of Arc2 and ring.

C_g relaxation time for other topologically modified architectures with their respective anisotropy values:

Architecture (Monomers)	Relaxation Time	Anisotropy
SP_model (500)	194.073	0.1159
Linear with side loops (190)	574.528	0.5323
Linearly attached rings (200)	339.425	0.3885
Flower_model (200)	109.757	0.2424
Arc2_2 (500)	295.458	0.1218

Table 7.4: Relaxation times and anisotropy for various architectures with different monomer counts.

7.2 C_E relaxation time data

The end-to-end vector relaxation time data for linear chain in comparison with C_g method and C_E are in the following table.

Monomers	**End-to-End Vector**	**Cg Relaxation Time**	**Eigenvector Relaxation**
100	1092	247	764
200	5130	1228	3432
300	12162	2982	8010
400	23754	5500	15317
500	38147	8525	24768

Table 7.5: C_E relaxation data for linear chains with varying monomer counts and methods.

The C_E relaxation time data for ring polymer and different ratios of Dumbbell polymers:

Monomers	**Ring Polymer**	**Dumbbell 1:1**	**Dumbbell 1:9**	**Dumbbell 1:4**	**Dumbbell 1:3**	**Dumbbell 3:7**
100	141	338	133	148	169	201
200	646	1379	612	661	748	855
300	1573	3050	1454	1601	1787	2040
400	2952	5614	2781	2921	3295	3843
500	4793	9652	4491	5208	5335	6152

Table 7.6: C_E relaxation data for ring polymers and dumbbell with varying ratios using eigenvector relaxation.

The C_E relaxation time data for ring polymer and different ratios of Arc1_2 polymers:

Monomers	Ring Polymer	Arc1_2 1:9	Arc1_2 3:7	Arc1_2 1:1	Arc1_2 7:3	Arc1_2 9:1
100	141	133	171	167	76	293
200	646	607	715	670	332	1116
300	1573	1449	1707	1562	798	2604
400	2952	2697	2995	2859	1508	4644
500	4793	4410	5134	4457	2410	7393

Table 7.7: C_E relaxation data for ring polymers and Arc1_2 ratios using eigenvector relaxation.

C_E relaxation time for other topologically modified architectures:

Architectures (Monomers)	Eigenvector Relaxation Time
SP_model (500)	756
Linear with side loops (190)	2013
Linearly attached rings (200)	1537
Flower_model (200)	359
Arc2_2 (500)	892

Table 7.8: C_E eigenvector relaxation times for various architectures

Now the data for C_E method which is displayed above is for the eigenvector associated with highest eigenvalue. But we have also performed similar analysis for eigenvectors associated with the middle and lowest eigenvalues. The next few tables and figures will represent data collected form the analysis of those eigenvectors.

The below table shows data for middle and lowest eigenvector for linear chain:

Monomers	**Highest**	**Middle**	**Lowest**
100	764	105	127
200	3432	441	535
300	8010	1024	1249
400	15317	1973	2347
500	24768	2935	3581

Table 7.9: Middle and lowest eigenvector relaxation linear

The below table shows data for middle and lowest eigenvector for ring polymer:

Monomers	**Highest**	**Middle**	**Lowest**
100	141	68	143
200	646	273	536
300	1573	632	1221
400	2952	1158	2188
500	4793	1881	3553

Table 7.10: Middle and lowest eigenvector relaxation ring

The table below shows the relaxation of the middle eigenvector using the C_E method for different ratios of Dumbbell polymer:

Monomers	Ring_Polymer	Dumbbell 1:1	Dumbbell 1:9	Dumbbell 1:4	Dumbbell 1:3	Dumbbell 3:7
100	68	44	66	63	62	62
200	273	172	263	246	242	231
300	632	388	594	557	542	518
400	1158	721	1090	1026	990	955
500	1881	1142	1706	1601	1588	1515

Table 7.11: Middle eigenvector relaxation

Figure 7.1 shows C_E relaxation time for middle eigenvectors against ratios of dumbbell with total 500 monomers:

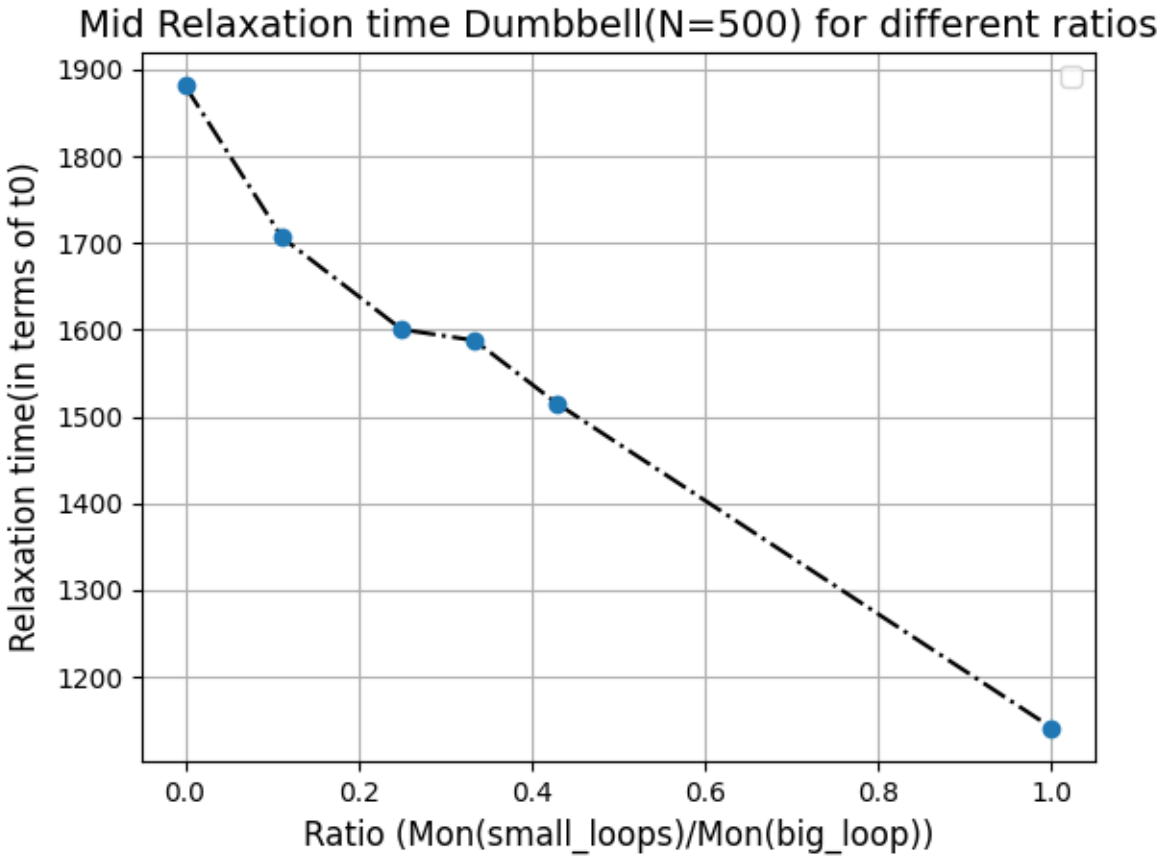

Figure 7.1: The graph shows C_E relaxation time for middle eigenvector for different ratios of Dumbbell polymer with 500 monomers.

The table below shows the relaxation of the lowest eigenvector using the C_E method for different ratios of Dumbbell polymer:

Monomers	**Ring_Polymer**	**Dumbbell 1:1**	**Dumbbell 1:9**	**Dumbbell 1:4**	**Dumbbell 1:3**	**Dumbbell 3:7**
100	143	49	137	121	109	96
200	536	194	513	450	408	356
300	1221	447	1148	1003	921	791
400	2188	834	2062	1787	1670	1430
500	3553	1327	3166	2860	2609	2321

Table 7.12: Lowest eigenvector relaxation

Figure 7.2 shows C_E relaxation time for lowest eigenvectors against ratios of dumbbell with total 500 monomers:

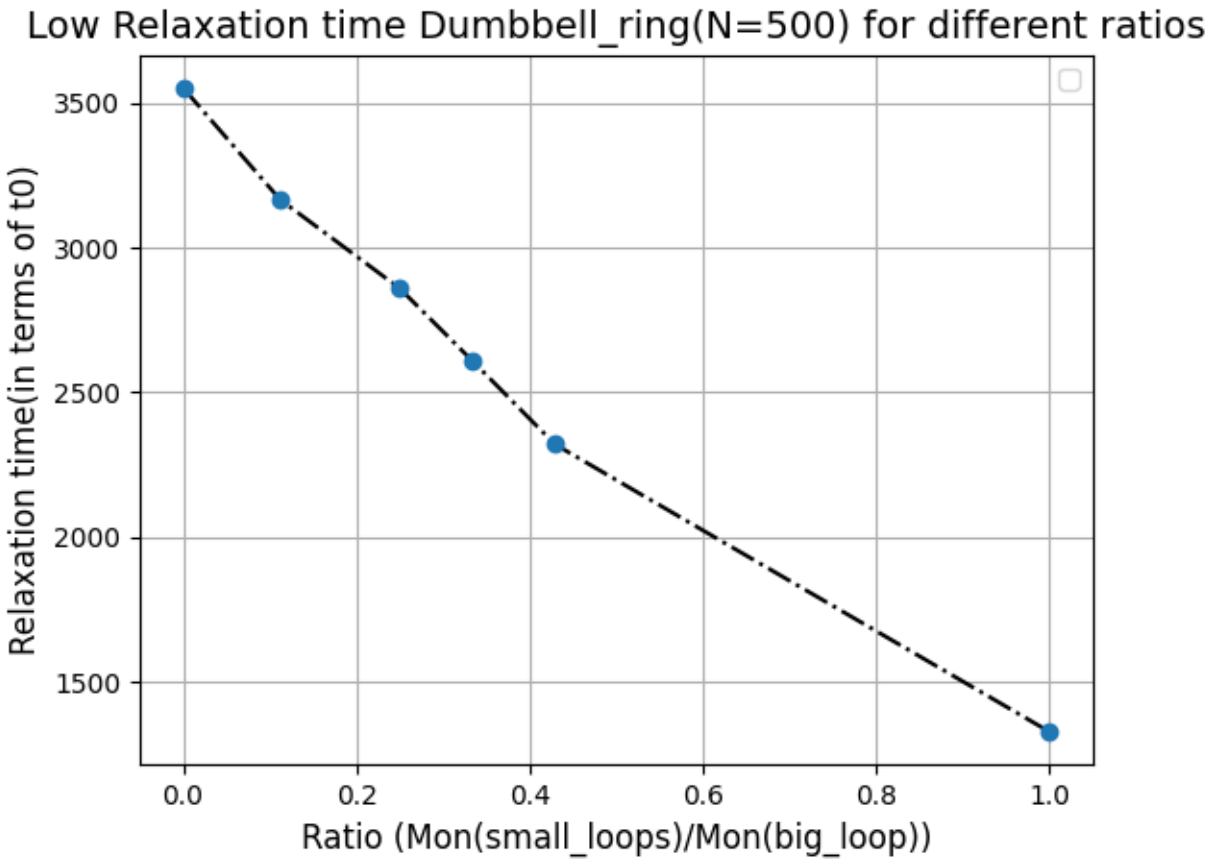

Figure 7.2: The graph shows C_E relaxation time for lowest eigenvector for different ratios of Dumbbell polymer with 500 monomers.

The table below shows the relaxation of the lowest eigenvector using the C_E method for different ratios of Arc1_2 polymer:

Monomers	**Ring_Polymer**	**Arc1_2 1:9**	**Arc1_2 3:7**	**Arc1_2 1:1**	**Arc1_2 7:3**	**Arc1_2 9:1**
100	143	135	99	58	89	45
200	536	517	365	221	318	180
300	1221	1152	830	490	698	413
400	2188	2069	1476	895	1247	776
500	3553	3287	2331	1440	1932	1207

Table 7.13: Lowest eigenvector relaxation

Figure 7.2 shows C_E relaxation time for lowest eigenvectors against ratios of Arc1_2 polymers with total 500 monomers:

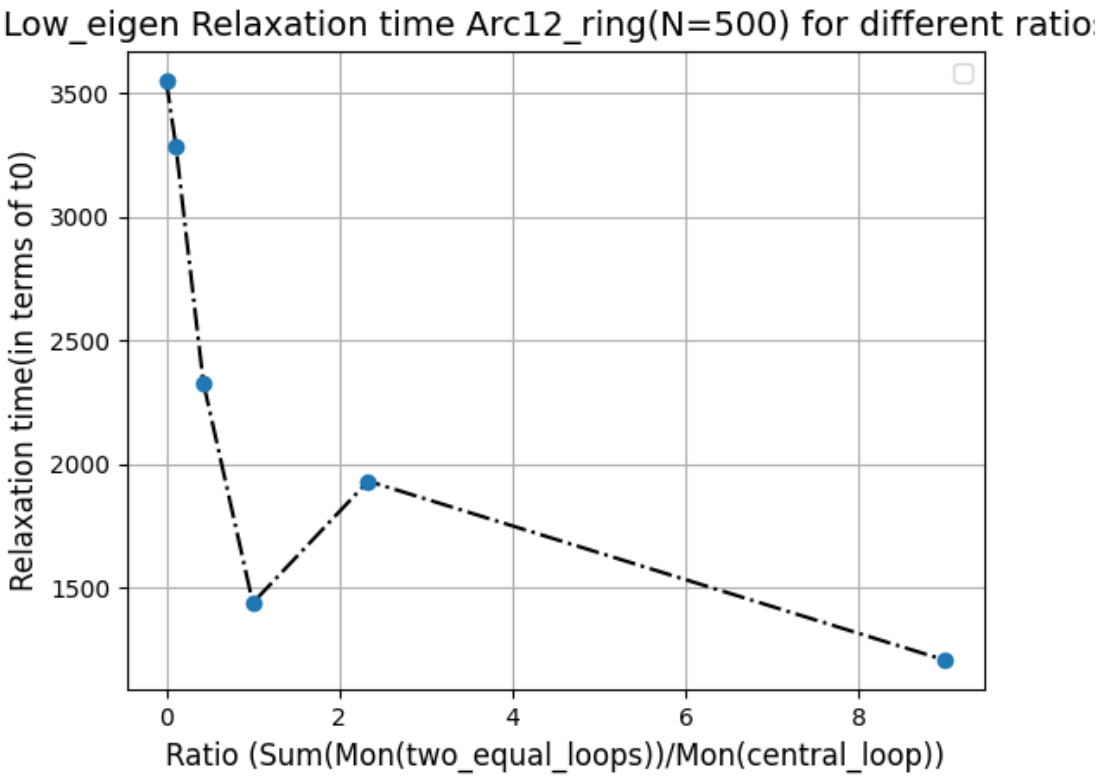

Figure 7.3: The graph shows C_E relaxation time for lowest eigenvector for different ratios of Arc1_2 polymer with 500 monomers.

The table below shows the relaxation of the middle eigenvector using the C_E method for different ratios of Arc1_2 polymer:

Monomers	**Ring_Polymer**	**Arc1_2 1:9**	**Arc1_2 3:7**	**Arc1_2 1:1**	**Arc1_2 7:3**	**Arc1_2 9:1**
100	68	65	58	42	37	40
200	273	261	217	159	141	155
300	632	602	496	353	323	351
400	1158	1084	883	635	581	649
500	1881	1745	1372	1033	911	1008

Table 7.14: Middle eigenvector relaxation

Figure 7.2 shows C_E relaxation time for lowest eigenvectors against ratios of Arc1_2 polymers with total 500 monomers:

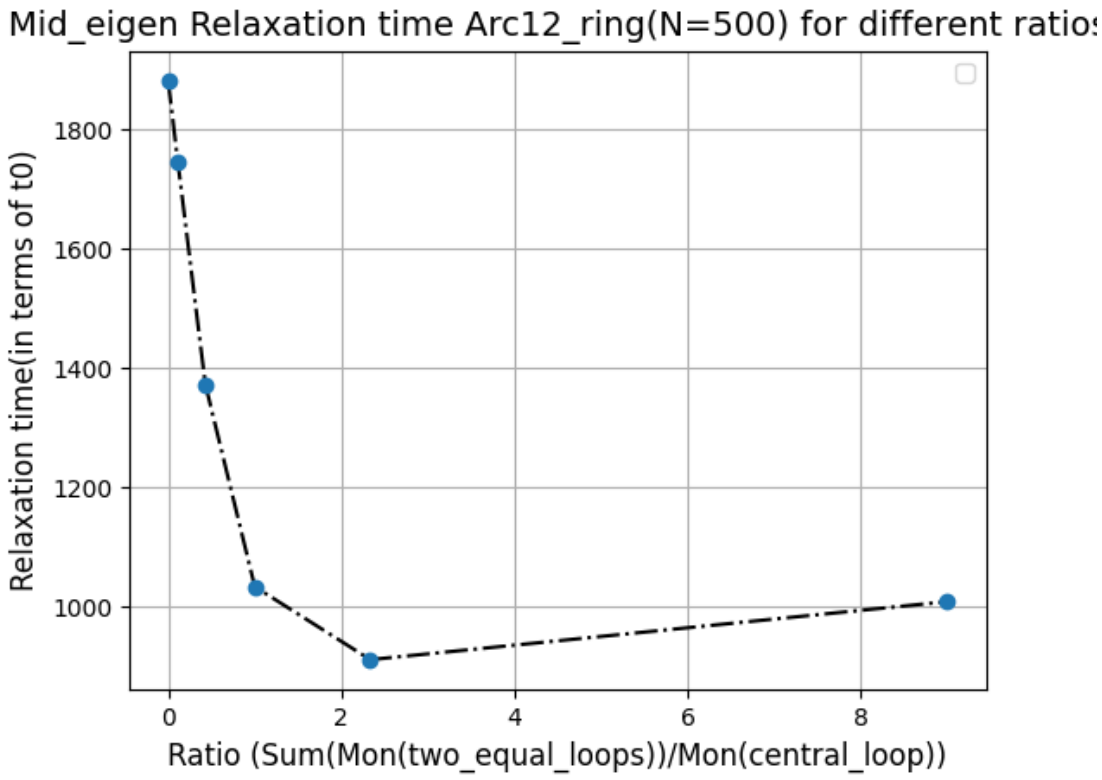

Figure 7.4: The graph shows C_E relaxation time for middle eigenvector for different ratios of Arc1_2 polymer with 500 monomers.

Below table shows both C_g and C_E relaxation time data for semiflexible polymer chain with different bending energy constants:

Monomers	Bending Constant	Cg_relaxation	Highest_eigen	Middle_eigen	Lowest_eigen	Anisotropy
200	50	10236.79	290021.84	9618.54	9705.36	0.870
200	100	8111.70	277984.40	9726.21	9766.76	0.872
200	200	8422.77	259696.32	9894.34	9906.75	0.869

Table 7.15: Relaxation of semiflexible polymer chains

7.3 Radius of Gyration data

The radius of gyration data for all the topologically modified polymers used in the thesis work with different lengths are summarized in the below table:

Topology	**N=100**	**N=200**	**N=300**	**N=400**	**N=500**
Linear Polymer	6.15	9.41	12.03	14.37	16.85
Ring Polymer	4.59	7.01	8.96	10.67	12.20
Symmetric Dumbbell	2.53	6.42	8.19	9.77	11.12
Dumbbell 10%	4.45	6.78	8.65	10.28	11.74
Dumbbell 20%	4.33	6.59	8.41	10.00	11.45
Dumbbell 25%	4.28	6.53	8.34	9.91	11.33
Dumbbell 30%	4.26	6.49	8.28	9.85	11.25
Symmetric Arc1_2	3.80	5.77	7.36	8.75	10.02
Arc1_2 1:9	4.40	6.73	8.61	10.21	11.68
Arc1_2 3:7	4.06	6.18	7.91	9.37	10.73
Arc1_2 7:3	3.71	5.63	7.18	8.53	9.74
Arc1_2 9:1	4.01	6.06	7.72	9.17	10.46

Table 7.16: R_g values for different polymer topologies

Topology (Monomers)	**R_g Values**
SP Model (500)	7.91
Arc2_2 (500)	8.61
Flower Model (200)	5.70
Linear Chain with Side Loops (190)	7.25
Linearly Attached Rings (200)	6.27

Table 7.17: Radius of gyration (R_g) values for other modified topologies

Bibliography

[1] Ralph H. Colby Michael Rubinstein. *Polymer Physics*. 2003.

[2] Axel Arnold, Behnaz Bozorgui, Daan Frenkel, Bae-Yeun Ha, and Suckjoon Jun. Unexpected relaxation dynamics of a self-avoiding polymer in cylindrical confinement. *The Journal of Chemical Physics*, 2007.

[3] Prabeen Kumar Pattnayak, Gaurav Tomar, and Aloke Kumar. Topology affects diffusion dynamics of ring polymers in dilute solutions, 2024.

[4] Kurt Kremer and Gary S. Grest. Dynamics of entangled linear polymer melts: a molecular-dynamics simulation. *The Journal of Chemical Physics*, 92(8):5057–5086, 04 1990.

[5] Kirill E. Polovnikov, Hugo B. Brandão, Sergey Belan, Bogdan Slavov, Maxim Imakaev, and Leonid A. Mirny. Crumpled polymer with loops recapitulates key features of chromosome organization. *Phys. Rev. X*, 13:041029, Nov 2023.

[6] Vaibhav Chaturvedi. Investigating the dynamics ofdifferent polymer architectures with modified topologies. Master's thesis, Indian Institute of Science Education and Research Pune, India, 2024.

[7] Debarshi Mitra, Shreerang Pande, and Apratim Chatterji. Topology-driven spatial organization of ring polymers under confinement. *Phys. Rev. E*, 106:054502, Nov 2022.